# MEGARA Exposure Time Calculator.

## Users Guide

**GTC Code:** EXT/UCM/1754-R

**Code:** TEC/MEG/057

**Issue:** 2.D

**Date:** 05/02/2016

**Pages:** 77

| | |
|---|---|
| **Authors:** | M. Carmen Eliche Moral |
| **Revised by:** | Ana Pérez Calpena<br>Nicolás Cardiel<br>África Castillo Morales<br>Alexandre Y. K. Bouquin |
| **Approved by:** | Armando Gil de Paz<br>Maria Luisa García Vargas |
| | |

**Distribution List:**

| Name | Affiliation | Date |
|---|---|---|
| MEGARA Instrument Team | | |
| MEGARA Science Team | | |
| GRANTECAN | | |

## Acronyms:

| | |
|---|---|
| AAO | Anglo-Australian Observatory |
| ADU | Analog to Digital Units |
| CAB | Centro de AstroBiología |
| CAHA | Centro Astronómico Hispano-Alemán |
| CCD | Charge-Coupled Device |
| CSS | Cascading Style Sheet |
| DAR | Differential Atmospheric Refraction |
| DC | Dark Current |
| DIT | Detector Integration Time |
| ESO | European Southern Observatory |
| ETC | Exposure Time Calculator |
| FC | Folded Cassegrain |
| FLAMES | Fibre Large Array Multi Element Spectrograph |
| FMPT | Fiber MOS Positioning Tool |
| FoV | Field of View |
| FRD | Focal Ratio Degradation |
| FWHM | Full Width at Half Maximum |
| GMOS | Gemini Multi-Object Spectrograph |
| GTC | Gran Telescopio Canarias |
| GTC-3M | Gran Telescopio CANARIAS 3 Mirrors |
| GUI | Graphical User Interface |
| GUAIX | Grupo Ucm de Astrofísica Instrumental y eXtragaláctica |
| HTML | Hypertext Markup Language |
| IAA | Instituto de Astrofísica de Andalucía |
| IAC | Instituto de Astrofísica de Canarias |
| IFS | Integral Field Spectroscopy |
| IFU | Integral Field Unit |
| INAOE | Instituto Nacional de Astrofísica, Óptica y Electrónica |
| JS | Javascript |
| LCB | Large Compact Bundle |
| MEGARA | Multi-Espectrógrafo en GTC de Alta Resolución para Astronomía |

| | |
|---|---|
| MOPSS | MEGARA Observing Preparation Software Suite |
| MOS | Multi-Object Spectroscopy / Multi-Object Spectrograph |
| NDIT | Number of DITs |
| NIR | Near InfraRed |
| OM | Observing Mode |
| OT | Observing Template |
| PPAK | Pmas fiber PacK |
| PS | Plate Scale |
| PSF | Point Spread Function |
| QE | Quantum Efficiency |
| RON | ReadOut Noise |
| RP | Robotic Positioner |
| RSS | Row Stacked Spectra |
| RUP | Rational Unified Process |
| SNR | Signal-to-noise ratio |
| TBC | To Be Confirmed |
| TBD | To Be Defined |
| UC | Use-Case |
| UCM | Universidad Complutense de Madrid |
| UML | Unified Modelling language |
| UPM | Universidad Politécnica de Madrid |
| URL | Universal Resource Locator |
| UVES | Ultraviolet and Visual Echelle Spectrograph |
| VLT | Very Large Telescope |
| VPH | Volume Phase Holographic grating |

## Change Control

| Issue | Date | Section | Page | Change description |
|---|---|---|---|---|
| 1.A | 31/05/2011 | All | All | First version of document. |
| 1.B | 29/09/2011 | | | GTC code and Reference Documents GTC codes added. |
| 1.C | 09/01/2012 | | | Section 3 "Overview":<br>– Updated Simulator number of packages and functionality associated to each of them.<br>Section "The Megara Simulator Tool":<br>– Changed the architecture of the Simulator. Now it is divided in the object simulator and the simulator.<br>Section "Flux transformation"<br>– Corrected equation XX. The Resolution R was used instead of the reciprocal dispersion. |
| 2.A | 15/03/2014 | All | All | – Simulator tool information removed from the present document to another one.<br>– Updated references in list.<br>– Included Summary (current Section 1).<br>– Updated section 2 according to design changes.<br>– Updated definitions in section 3. Inserted definition of voxel. Corrected definition of spaxel throughout the text.<br>– All sections updated according to current modifications to ETC.<br>– Updated outputs in 7.3.<br>– Comments on present status of the tool (CDR version) distributed throughout the text.<br>– Revised text of model equations.<br>– New figures with transmission profiles updated to CDR: 3, 4, 6, 8, 9, and 10.<br>– Updated estimates in Table 10 with current ETC prototype version.<br>– Updated Tables throughout the manuscript. |
| 2.B | 31/07/2014 | <br>-<br>7.1<br>7.2.4<br>7.2.5 | <br>1,3<br>41<br>44,45<br>45 | Revised CDR issue according to comment:<br>CDR-INT-000<br>CDR-INT-158<br>CDR-INT-160<br>CDR-INT-161<br>CDR-INT-157 (Acronym added) |
| | | | | |

| | | | | |
|---|---|---|---|---|
| 2.C | 26/01/2015 | All | All | References to the SCB fiber bundle are deleted.<br>Section 5 has been updated describing the installation |
| 2.D | 05/02/2016 | All | All | Sections have been updated according to the new version online |

## Applicable (A) and Reference (R) Documents

| Nº | Document Name | Code |
|---|---|---|
| R.1 | Rational Unified Process 5.1 | No code |
| R.2 | *"The Unified Modelling Language"*. Version 1.1 - Object Management Group | No code |
| R.3 | *"UML for Managers"*. Jason Gorman 2005<br>e-book available at:<br>http://www.codemanship.co.uk/parlezuml/e-books/umlformanagers/ | No code |
| R.4 | MEGARA Functional Requirements Document | RQ/IN-MG/001 |
| R.5 | MEGARA Conceptual Design. Overview | TEC/MEG/009 |
| R.6 | MEGARA. Feasibility study for an intermediate resolution spectrograph for the GTC | TEC/MEG/001 |
| R.7 | GTC Services to the Instruments (DCI/INST/0053-R) | GTC/MEG/007 |
| R.8 | Science Instruments - Support Elements (DCI/STMA/0037-R) | GTC/MEG/010 |
| R.9 | Folded Cassegrain Instrument Rotator - Science Instrument (DCI/TELE/0057-R) | GTC/MEG/002 |
| R.10 | Interface Folded Cassegrain Instrument Rotator - Instrument (Drawing) (DR-I-IN-TL-007/001) | GTC/MEG/011 |
| R.11 | Instrumentation - Telescope Structure (DCI/STMA/0018-R) | GTC/MEG/009 |
| R.12 | MEGARA Fiber MOS Conceptual Design | TEC/MEG/016 |
| R.13 | "*Communication in the presence of noise*", C.E. Shanon, 1949. Proc. Institute of Radio Engineers, vol. 37, no. 1, pp. 10-21 | No code |
| R.14 | GTC Control System Software Standards (ESP/CTRL/0045-R) | GTC/MEG/004 |
| R.15 | MEGARA Observing Modes | TEC/MEG/005 |
| R.16 | FRIDA Operational Concepts Definitions, Issue 2.B | FR/UR-SC/007 |
| R.17 | Sánchez, S. F. : '*E3D, the Euro3D visualization tool I: Description of the program and its capabilities*'. 2004, AN, 325, 167. | No code |
| R.18 | Sánchez, S. F.: '*Techniques for reducing fiber-fed and integral-field spectroscopy data: An implementation on R3D*'. 2006, AN, 327, 850 | No code |
| R.19 | "*Volume Phase Holographic Gratings*". S. Barden, 1998. NOAO Newsletter - Number 54 | No code |
| R.20 | "*Optical Astronomical Instrumentation*". S. Barden, J. Arns, & B. Colburn, 1998, Ed.: Sandro D'Odorico, Proc. SPIE, Vol. 3355, p. 866-876 | No code |
| R.21 | MEGARA Control System. Stakeholder Needs (III). Observing Program Management System | TEC/MEG/036 |
| R.22 | MEGARA Control System - Use Cases Model Survey (III). Observing Program Management Subsystem (OPMS) | TEC/MEG/040 |

| | | |
|---|---|---|
| R.23 | "*Exposure Time Calculators – Formula Book*". A. Modigliani, 2009 | No code |
| R.24 | "*La Palma night-sky brightness*". C.R.Benn & S.L. Ellison, 1997. La Palma technical note 115 | No code |
| R.25 | "*The Definition of Dark, Grey and Bright Time at ING*". I. Skillen, 2002. ING Technical Note 127. | No code |
| R.26 | *"Exposure Time Calculator for LUCIFER – User Manual*". A. Germeroth, 2009 | No code |
| R.27 | "*Tech Note: Pixel Response Effects on CCD Camera Gain Calibration*", M. Newberry, 1998. Mirametrics, Inc. | No code |
| R.28 | GMOS integration time calculator. M. Dillman, 2009. http://sciopsedit.gemini.edu/sciops/instruments/integration-time-calculators/gmosn-itc | No code |
| R.29 | CAHA/PMAS exposure time calculator. S. Sánchez, 2006. http://www.caha.es/sanchez/pmas/calculator/pmas_etc.php | No code |
| R.30 | GIRAFFE Exposure Time Calculator, versión 3.2.7ª (March 4, 2009). http://www.eso.org/observing/etc/bin/gen/forms?INS.NAME=GIRAFFE++INS.MODE=spectro | No code |
| R.31 | "*Absolute flux calibrated spectrum of Vega*". L. Colina, R. Bohlin, & F. Castelli, 1996. Instrument Science Report, CAL/SCS-008 | No code |
| R.32 | Bessel, M. S. 1990, PASP, 91, 589 | No code |
| R.33 | Bessel, M. S. 1983, PASP, 95, 480 | No code |
| R.34 | Bessel, M. S. 1990, PASP, 102, 1181 | No code |
| R.35 | Transmission curves of Johnson-Bessel filters of TCS/CAMELOT. http://www.iac.es/telescopes/tcs/filtros-eng.htm | No code |
| R.36 | *Transparency of sky at Mauna Kea in optical range*. Lord, S.D., NASA Tech. Mem. 103957, and Gemini Observatory. http://www.gemini.edu/sciops/ObsProcess/obsConstraints/ocTransparency.html#MK%20optical%20extinction%20curve | No code |

| | | |
|---|---|---|
| R.37 | "*Study of the photon flux from the night sky at La Palma and Namibia, in the wavelength relevant for imaging atmospheric Cherenkov telescopes*" S. Preu, G. Hermann, W. Holfmann, and A. Kohnle. Nuclear Instruments and Methods in Physics Research, Section A, Volume 481, Issue 1-3, pp. 229-240 | No code |
| R.38 | OSIRIS Exposure Time Calculator. J. Ignacio González Serrano, 2010. http://venus.ifca.unican.es/~gserrano/osiris/Calculators.html | No code |
| R.39 | MEGARA Spectrograph Conceptual Design | TEC/MEG/006 |
| R.40 | MEGARA Detector and DAS Preliminary Design | MEG/TEC/051 |
| R.41 | "*The Importance of Atmospheric Differential Refraction in Spectrophotometry*". Filippenko, A. V. 1982, PASP, 94, 715 | No code |
| R.42 | *"Spherical astronomy"*. Green, R.M. 1985, Cambridge University, p.87 | No code |
| R.43 | "*An Accurate Method for Computing Atmospheric Refraction*". Stone, R.C., 1996, PASP 108,1051 | No code |
| R.44 | *"Atmospheric refraction and slit transmission*". S. Pedraz, 2003.http://www.caha.es/newsletter/news03b/pedraz/newslet.html | No code |
| R.45 | "*Optical Refractive Index of Air: Dependence on Pressure, Temperature and Composition*"**.** Owens, J.C., 1967, Appl.Opt. 6, 51 | No code |
| R.46 | "*E2V CCD231-84 Back Illuminated Scientific CCD Sensor*" Document description.E2V Technologies (UK) limited, 2009. A1A-765136 Version 2 (July 2009). http://www.e2v.com | No code |
| R.47 | "MEGARA PSF Simulations: Spectral Resolution and Cross-talk effects." | TEC/MEG/076 |
| R.48 | "MEGARA Preliminary Design: Instrument Overview" | TEC/MEG/059 |
| R.49 | MEGARA Detailed Design: Flux Homogeneity, Issue 1.B | TEC/MEG/117 |
| R.50 | *FITS: A Flexible Image Transport System*, Wells, D. C., Greisen, E. W., and Harten, R. H., 1981. A&AS, 44, 363 | No code |
| R.51 | MEGARA Detailed design: Instrument Overview, Issue 1.A | TEC/MEG/106 |

| | | |
|---|---|---|
| R.52 | MEGARA Detailed Design:Transmission, Issue 1.C | TEC/MEG/055 |
| R.53 | RGO/La Palma Technical Note no. 31, Atmospheric *Extinction at the Roque de los Muchachos Observatory, La Palma*, D L King (RGO), 6 September 1985 | No code |
| | | |

## Applicable (A) and Reference (R) Documents (GTC codes)

| Nº | Document Name | Code |
|---|---|---|
| R.1 | Rational Unified Process 5.1 | No code |
| R.2 | *"The Unified Modelling Language"*. Version 1.1 - Object Management Group | No code |
| R.3 | *"UML for Managers*". Jason Gorman 2005<br>e-book available at:<br>http://www.codemanship.co.uk/parlezuml/e-books/umlformanagers/ | No code |
| R.4 | MEGARA Functional Requirements Document | EXT/UCM/1711-R |
| R.5 | MEGARA Conceptual Design. Overview | No code |
| R.6 | MEGARA. Feasibility study for an intermediate resolution spectrograph for the GTC | No code |
| R.7 | GTC Services to the Instruments (DCI/INST/0053-R) | DCI/INST/0053-R |
| R.8 | Science Instruments - Support Elements (DCI/STMA/0037-R) | DCI/STMA/0037-R |
| R.9 | Folded Cassegrain Instrument Rotator - Science Instrument (DCI/TELE/0057-R) | DCI/TELE/0057-R |
| R.10 | Interface Folded Cassegrain Instrument Rotator - Instrument (Drawing) (DR-I-IN-TL-007/001) | DR-I-IN-TL-007/001 |
| R.11 | Instrumentation - Telescope Structure (DCI/STMA/0018-R) | DCI/STMA/0018-R |
| R.12 | MEGARA Fiber MOS Conceptual Design | No code |
| R.13 | "*Communication in the presence of noise*", C.E. Shanon, 1949. Proc. Institute of Radio Engineers, vol. 37, no. 1, pp. 10-21 | No code |
| R.14 | GTC Control System Software Standards (ESP/CTRL/0045-R) | ESP/CTRL/0045-R |
| R.15 | MEGARA Observing Modes | EXT/UCM/1714-R |
| R.16 | FRIDA Operational Concepts Definitions, Issue 2.B | No code |
| R.17 | Sánchez, S. F. : '*E3D, the Euro3D visualization tool I: Description of the program and its capabilities*'. 2004, AN, 325, 167. | No code |
| R.18 | Sánchez, S. F.: '*Techniques for reducing fiber-fed and integral-field spectroscopy data: An implementation on R3D*'. 2006, AN, 327, 850 | No code |
| R.19 | "*Volume Phase Holographic Gratings*". S. Barden, 1998. NOAO Newsletter - Number 54 | No code |
| R.20 | "*Optical Astronomical Instrumentation*". S. Barden, J. Arns, & B. Colburn, 1998, Ed.: Sandro D'Odorico, Proc. SPIE, Vol. 3355, p. 866-876 | No code |
| R.21 | MEGARA Control System. Stakeholder Needs (III). Observing Program Management System | EXT/UCM/1747-R |
| R.22 | MEGARA Control System - Use Cases Model Survey (III). Observing Program Management Subsystem (OPMS) | EXT/UCM/1751-R |

| | | |
|---|---|---|
| R.23 | "*Exposure Time Calculators – Formula Book*". A. Modigliani, 2009 | No code |
| R.24 | "*La Palma night-sky brightness*". C.R.Benn & S.L. Ellison, 1997. La Palma technical note 115 | No code |
| R.25 | "*The Definition of Dark, Grey and Bright Time at ING*". I. Skillen, 2002. ING Technical Note 127. | No code |
| R.26 | *"Exposure Time Calculator for LUCIFER – User Manual*". A. Germeroth, 2009 | No code |
| R.27 | "*Tech Note: Pixel Response Effects on CCD Camera Gain Calibration*", M. Newberry, 1998. Mirametrics, Inc. | No code |
| R.28 | GMOS integration time calculator. M. Dillman, 2009. http://sciopsedit.gemini.edu/sciops/instruments/integration-time-calculators/gmosn-itc | No code |
| R.29 | CAHA/PMAS exposure time calculator. S. Sánchez, 2006. http://www.caha.es/sanchez/pmas/calculator/pmas_etc.php | No code |
| R.30 | GIRAFFE Exposure Time Calculator, versión 3.2.7ª (March 4, 2009). http://www.eso.org/observing/etc/bin/gen/forms?INS.NAME=GIRAFFE++INS.MODE=spectro | No code |
| R.31 | "*Absolute flux calibrated spectrum of Vega*". L. Colina, R. Bohlin, & F. Castelli, 1996. Instrument Science Report, CAL/SCS-008 | No code |
| R.32 | Bessel, M. S. 1990, PASP, 91, 589 | No code |
| R.33 | Bessel, M. S. 1983, PASP, 95, 480 | No code |
| R.34 | Bessel, M. S. 1990, PASP, 102, 1181 | No code |
| R.35 | Transmission curves of Johnson-Bessel filters of TCS/CAMELOT. http://www.iac.es/telescopes/tcs/filtros-eng.htm | No code |
| R.36 | *Transparency of sky at Mauna Kea in optical range*. Lord, S.D., NASA Tech. Mem. 103957, and Gemini Observatory. http://www.gemini.edu/sciops/ObsProcess/obsConstraints/ocTransparency.html#MK%20optical%20extinction%20curve | No code |

| | | |
|---|---|---|
| R.37 | "*Study of the photon flux from the night sky at La Palma and Namibia, in the wavelength relevant for imaging atmospheric Cherenkov telescopes*" S. Preu, G. Hermann, W. Holfmann, and A. Kohnle. Nuclear Instruments and Methods in Physics Research, Section A, Volume 481, Issue 1-3, pp. 229-240 | No code |
| R.38 | OSIRIS Exposure Time Calculator. J. Ignacio González Serrano, 2010. http://venus.ifca.unican.es/~gserrano/osiris/Calculators.html | No code |
| R.39 | MEGARA Spectrograph Conceptual Design | No code |
| R.40 | MEGARA Detector and DAS Preliminary Design | EXT/UCM/1737-R |
| R.41 | "*The Importance of Atmospheric Differential Refraction in Spectrophotometry*". Filippenko, A. V. 1982, PASP, 94, 715 | No code |
| R.42 | *"Spherical astronomy"*. Green, R.M. 1985, Cambridge University, p.87 | No code |
| R.43 | "*An Accurate Method for Computing Atmospheric Refraction*". Stone, R.C., 1996, PASP 108,1051 | No code |
| R.44 | *"Atmospheric refraction and slit transmission*". S. Pedraz, 2003.http://www.caha.es/newsletter/news03b/pedraz/newslet.html | No code |
| R.45 | "*Optical Refractive Index of Air: Dependence on Pressure, Temperature and Composition*". Owens, J.C., 1967, Appl.Opt. 6, 51 | No code |
| R.46 | "*E2V CCD231-84 Back Illuminated Scientific CCD Sensor*" Document description. E2V Technologies (UK) limited, 2009. A1A-765136 Version 2 (July 2009). http://www.e2v.com | No code |
| R.47 | "MEGARA PSF Simulations: Spectral Resolution and Cross-talk effects." | No code |
| R.48 | "MEGARA Preliminary Design: Instrument Overview" | EXT/UCM/1778-R |
| R.49 | MEGARA Detailed Design: Flux Homogeneity, Issue 1.B | TBD |
| R.50 | *FITS: A Flexible Image Transport System*, Wells, D. C., Greisen, E. W., and Harten, R. H., 1981. A&AS, 44, 363 | No code |
| R.51 | MEGARA Detailed design: Instrument Overview, Issue 1.A | TBD |

| | | |
|---|---|---|
| R.52 | MEGARA Detailed Design:Transmission, Issue 1.C | EXT/UCM/1741-R |
| R.53 | RGO/La Palma Technical Note no. 31, Atmospheric *Extinction at the Roque de los Muchachos Observatory, La Palma*, D L King (RGO), 6 September 1985 | No code |
| | | |

# INDEX

## 1. SUMMARY

This document presents the Users Guide of a software component of the MEGARA Observing Preparation Software Suite (MOPSS hereafter): the MEGARA Exposure Time Calculator (ETC). The MOPSS shall provide the tools needed to assist observers to plan their observations in an optimum way. In the following sections, a detailed description of the physical model of the MEGARA ETC and its usage is provided.

The MEGARA ETC is originaly a stand-alone software package that has now been ported to an online-accessible version. A prototype of this tool has already been implemented to facilitate the definition and assessment of the MEGARA Science Cases. Newer versions of it are being developed at this time to incorporate the instrument updates and changes as the project advances [R.5, R.14]. Therefore, this document will be thoroughly updated.

## 2. INTRODUCTION

MEGARA (Multi-Espectrógrafo en GTC de Alta Resolución para Astronomía) is an optical Integral-Field Unit (IFU) and Multi-Object Spectrograph (MOS) designed for the GTC 10.4m telescope in La Palma.

The MEGARA IFU mode will offer a fiber bundle covering 12.5x11.3 arcsec$^2$ with a spaxel size of 0.62 arcsec (Large Compact Bundle; LCB, which uses 100μm-core optical fibers).

The MEGARA MOS will allow observing up to 100 objects in a region of 3.5' x 3.5' around the IFU bundle [R.4-R.6]. Eight of these bundles will be devoted to the determination of the sky during the observation with the LCB IFU. Each of the MEGARA MOS positioners can place a mini-bundle of 7 fibers (1.6" of diameter in total on the sky). The positioning of the fiber optical bundle is performed by combining the interpolation of two rotations. The interpolation between rotation 1 and rotation 2 allows covering the patrol area assigned to each robotic positioner.

The IFUs and the robotic positioners (RPs) along will the interface with the optical fibers will be placed at the Folded-Cassegrain focus of the GTC 10.4-m telescope.

In the case of the MEGARA Spectrograph the optical elements are placed on an optical table. Apart from the "baseline" optical elements, such as the collimator and the camera, there is a mechanism that automatically interchanges 11 Volume Phase Holographic gratings (VPHs), a mechanism that provides focus adjustment, a mechanism that allows switching between pseudo-slits and a rotating shutter.

MEGARA will use VPHs as dispersive elements [R.4-R.7]. The wavelength coverage will be 3,650-10,000 Å, with a spectral resolving power from 6,000 to 18,700 in the LCB and MOS modes, depending on the set of VPHs available at the VPH Wheel. The whole optical spectrum will be covered at low resolution, or at medium and high resolutions depending on this.

MEGARA is a collaborative project of an international consortium comprising:

1. The Universidad Complutense de Madrid (UCM, Spain), as the leading institution.

2. The Instituto Nacional de Astrofísica, Óptica y Electrónica (INAOE, México).

3. The Instituto de Astrofísica de Andalucía (IAA-CSIC, Spain).

4. The Universidad Politécnica de Madrid (UPM, Spain).

Main private contractors are FRACTAL (Spain), AVS (Spain), GMV (Spain), Wasatch Photonics (USA), and SEDI (France).

The MEGARA ETC, the Simulator, the MEGARA Fiber MOS Assignment Tool (FMAT) and the MEGARA Fiber MOS Positioning Tool (FMPT) are software packages contained in the MOPSS system. The MOPSS shall provide the tools needed to assist observers to plan their observations in an optimum way. In the following sections, relevant information to the user of the ETC is provided.

The main objectives of each tool are the following:

1. The MEGARA ETC tool is intended to simulate the signal-to-noise ratio (SNR) that would be obtained for the continuum or for a specific emission line of an input source. The tool is intended to derive also the change in SNR vs. wavelength in the case that a source spectrum from the database is provided as input, in one voxel or from one or several spaxels. The tool can also estimate the limiting magnitude of flux of a line or the continuum for an input SNR and exposure time, as well as the exposure time to get a final SNR on a given source line or continuum.

2. The MEGARA Simulator tool is intended to create a set of images simulating the output of the MEGARA instrument depending on the observational strategy for a given input source. The tool includes the expected sky contribution to the final spectrum, considers the wavelength range of the selected MEGARA configuration, and simulates the output observation of the provided input source as a function of the input observational parameters chosen by the user. The Simulator returns a MEGARA frame in FITS format with the simulated spectra corresponding to each spaxel from any input flux calibrated spectrum.

3. The FMAT will determine the optimal assignment of RPs for an input list of source coordinates in the 3.5x3.5 arcmin$^2$ MEGARA FoV to cover as many sources as possible; the FMPT will estimate the movements to be done by the RPs (simultaneous and subsequent) to ensure no collisions among adjacent positioners while minimizing the time to configure all of them.

The former two tools must account for the flux distribution of the input source, the instrument configuration, and the atmospheric conditions of the run, as well as for the observation strategy to use.

This document presents the Users Guide of the MEGARA ETC.

## 3. DEFINITIONS

### 3.1. Airmass

Airmass is a dimensionless parameter related to zenital angle z (which is the arc of a vertical circle between the zenith and the target's position on the celestial sphere, measured from the zenith through 90º). Airmass is just sec(z)=1/cos(z), and it is related to the amount of atmosphere that the ray of light has to cross in plan-parallel approximation. For zenith (z=0º), its value is one (where the absorption is minimum), and increases to infinite at the horizon (z=90º), where the absorption is maximum (but not infinity, as the plane-parallel approximation is no longer valid).

### 3.2. Bias Frame

The value of the pixels of a CCD image with zero exposure time include an offset inserted to avoid negative mean levels of all pixels in the image (also known as mean bias level or sometimes simply bias level), an individual pixel-to-pixel variation (that corresponds to changes in the bias level), and the readout noise (§3.18). A bias frame is the CCD image resulting from a direct readout of the detector with an exposure time set to zero and no illumination (i.e., with the shutter behind the pseudo-slit of the spectrograph closed).

### 3.3. Detector Integration Time (DIT)

It is the integration time (in seconds) needed to obtain a detector frame.

### 3.4. Fiber

A MEGARA fiber has a circular core section of 100μm. The fiber is appended to a micro-lens with a hexagonal section exposed to the light, responsible of changing the focal ratio coming from the telescope to the one required by the instrument [R.5, R.12]. The hexagonal section of the micro-lens is inscribed in a circle of projected diameter $D_{eff}$ = 0.62 arcsec in the LCB and MOS (see the definition of *spaxel* in §3.20). The side of the hexagon $L_{spaxel}$ is equal to the radius of the circle (see *Figure 1*). The distance between the centers of adjacent microlenses is two times the apothem (a). The fiber is appended to this hexagonal region that is being over-illuminated to ensure a uniform illumination in the whole circular section of the fiber and a homogeneous illumination from fiber to fiber. This is to the penalty of small light losses, which imply an effective transmission of 83.5% for the 100μm-core fibers [R.48] [R.49].

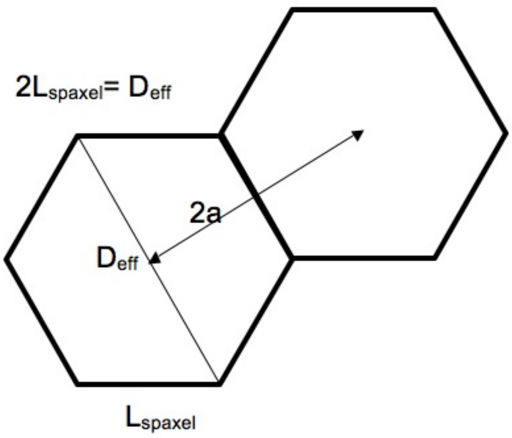


***Figure 1:*** *Layout of two MEGARA micro-lenses. The circular fiber is behind each hexagonal region, at a given distance, being over-illuminated [R.49]. The distance between centers is twice the apothem.*

### 3.5. Flatfield Frame

It is a frame taken with a uniform illumination. It contains information about:

- Photo-Response Non-Uniformity.
- Vignetting of optical elements.
- Interference fringing within detector.
- Cosmetic defects (dark pixels or columns).
- Contamination (dust near focal plane or optical train).
- Thermal emission of the telescope plus the instrument system.

### 3.6. Frame

A frame (or image) is the number matrix resulting from reading the CCD pixels after a given exposure of it. This matrix is usually saved into a FITS file format [R.50].

### 3.7. Linear Dispersion

The linear dispersion associates wavelengths and positions of the lines in a spectrum. In MEGARA, due to distortions related with the dispersive elements, the relationship between the wavelength of the spectral lines and the positions they appear in is not linear. In order to take this into account and perform the wavelength calibration, an *n*-degree polynomial is used (with *n* typically 3 or 5).

$$\lambda(x) = \sum_{i=0}^{n} a_i x^i \quad . (1)$$

The ETC does not account for this effect, as it does not consider other effects typical of CCD frames, such as bias, flat-field or vignetting, but it considers the change in linear dispersion at each wavelength for each VPH (the linear dispersion changes slightly across the wavelength range of the VPHs to keep the spectral FWHM constant by design [R.51]).

## 3.8. Nyquist-Shanon theorem

A fundamental result in the field of information theory, in particular in signal processing, is the Nyquist-Shanon theorem, which in its Shanon's version states that [R.13]: "If a function *x(t)* contains no frequencies higher than *B* hertz, it is completely determined by giving its ordinates at a series of points spaced *1/(2B)* seconds apart".

Translated to the spatial sampling of a signal in the detector plane, the previous theorem implies that, in the case that the minimum resolution element of the detector is a pixel length in each detector dimension, at least 2 pixels in each detector dimension are required in order to sample correctly the input signal. So, in this case, the minimum resolution element on the detector would be 2×2.

In the case of MEGARA, this theorem states somehow differently, accounting for the fact that the minimum spatial resolution element is the projection of one fibre (4 pixels), and the minimum spectral resolution element is set by the FWHM of each VPH (4 pixels, [R.51]. If each resolution element is sampled with at least 2 pixels, the Nyquist-Shanon theorem is fulfilled. Consult §3.20 for more details.

## 3.9. Number of DITs (NDIT)

It is the number of independent detector frames (each of DIT seconds) obtained sequentially at a fixed position.

## 3.10. Observing Strategy

Using the same GTC/MEGARA configuration, data can be taken in different ways to reduce the overheads, get sky measurements, cover gaps in the exposure frames, facilitate the reduction process, or improve the quality of the obtained calibrations. We will refer to these ways of obtaining data in order to fit some specific observational requirements as "observing strategies".

Besides, MEGARA will offer three general scientific OMs: exposing only the LCB IFU in normal and fast-mapping modes ("LCB IFU scientific observation" and "LCB IFU fast mapping"), and the RPs ("Fiber MOS scientific observation") [R.15]. Each OM has its own general Observing Template (OT), which consists on a standard series of orders and parameters that are executed by the Sequencer to stablish the adequate configuration of the telescope, the instrument, and the auxiliary systems to take a frame in the selected OM.

The sequences for the fast-mapping modes include the required actions to obtain scientifically-valid data with the LCB IFU instrument mode of MEGARA covering a relatively large area of the sky (of an extension equivalent to several LCB FoV).

Sometimes, it is useful to make specific realizations of a given general OT to implement a given observing strategy and use it during several observing runs. These specific implementations of one of the general OTs give place to other secondary OMs. Therefore, each OM has its own general OT and, in some cases, additional associated OTs for implementing specific observing strategies.

## 3.11. Operation Modes

From [R.16], an operation or observing mode (OM) is a data taking activity or data taking preparation activity with the telescope, instrument (in this case, MEGARA), and control system at certain established configurations, which are intrinsically associated to this OM.

The OMs that are required for the MEGARA control system in order to carry out observations with MEGARA include calibration, auxiliary, and scientific templates [R.15]. The MEGARA ETC shall implement the characteristics of the basic scientific OMs offered by MEGARA at each status of the project to estimate SNRs and exposure times.

## 3.12. Point spread function

The PSF is the flux distribution figure generated by the atmosphere+telescope+instrument system on the detector plane from a point-like signal.

## 3.13. Pseudo-slit

The MEGARA spectrograph has three interchangeable pseudo-slits, which can accommodate up to 650 fibers placed simulating a long slit of 119 mm length in each of them. Although the conceptual design allowed a total of ~700 fibers, a realistic design of the pseudo-slit suggests a maximum number of fibers of ~650. In MEGARA a mechanism will ex-change the pseudo-slit in place for the LCB IFU and MOS modes respectively. The pseudo-slit of the LCB IFU will contain the fibers coming from 8 external RPs at the edges of the MOS field (i.e., 56 fibers) to facilitate the simultaneous acquisition of sky spectra with the LCB IFU [R.51].

## 3.14. Quantum efficiency

Quantum efficiency (QE) is the percentage of photons to be received by the detector that will produce an electron-hole pair. The MEGARA detector is the CCD231-84 (layer Astro AR Mult-2) [R.52].

## 3.15. Raw Data

Data as are retrieved from the detector, without any reduction.

## 3.16. Roboctic Positioner

The robotic positioner refers to each individual mechanical device of the Fiber MOS that is dedicated to put the fiber mini-bundle (which is composed by 7 fibers) at any position of the corresponding patrol area. The reference position for each positioner is the center of the central fiber of the 7-fiber mini-bundle.

The positioning of the fiber optical bundle is performed by combining the interpolation of two rotations. The interpolation between rotation 1 (R1) and rotation 2 (R2) allows covering the area assigned to each positioner.

## 3.17. Row stacked spectra

Row stacked spectra format (or RSS format) consists on a 2D FITS image in which the X-axis corresponds to the dispersion axis, and the other one corresponds to a given spatial ordering of the spectra determined by a position table [R.16, R.17]. Therefore, each RSS FITS file has an associated position table, which indicates the spaxel that corresponds to the Nth spectrum found in the Y-axis of the RSS FITS. In all the UML diagrams describing the MEGARA ETC and Simulator, the classes associated to RSS have a coordinate file associated to them.

Note that the spectra in a RSS frame correspond to the spectra of each spaxel. They are obtained by collapsing the spectra in the spatial direction of the CCD frame. In MEGARA, each fiber is projected onto 4 pixels in the spatial direction of the detector in all configurations by design in raw data (we will call them CCD frames). So, we will distinguish between RSS frames and CCD frames format henceforth.

The number of spectra in the RSS frames is equal to the number of fibers placed on the pseudo-slit that is being used (623 for the LCB and 644 for the MOS mode).

The MEGARA ETC will estimate global SNR per spaxel (i.e., integrated for all wavelengths in the corresponding expected ideal spectrum of the spaxel), as well as SNR in several rings of spaxels when the considered FWHM in the sky distributes the light of a point source in more than one spaxel, according to the simulations of flux homogeneity and distribution performed for the instrument [R.49].

## 3.18. Readout noise

The ReadOut Noise (RON) is the noise of a pixel in an image coming from the amplifier electronics attached to the CCD. It is included whenever the CCD is read. For MEGARA, it is ~2.8 electrons per pixel [R.51].

## 3.19. Spatial resolution

See §§3.8 and 3.20.

## 3.20. Spaxel

Minimum resolution element on the sky resolved by the different modes of MEGARA. The MEGARA spaxels are hexagonal shaped and have sizes of 0.62 arcsec for the LCB and MOS [R51]. These sizes correspond to the diameter of the circle on which the hexagonal spaxel is inscribed (see Figure 1).

## 3.21. Voxel

Minimum spectral and spatial resolution element in the detector plane of MEGARA for a given single wavelength. This corresponds to the projection of a single fiber at a given single wavelength onto the detector. This is ~4 pixels (3.6 pixels FWHM for LCB and MOS) both along the spatial and spectral (for a single wavelength) directions. The size of this projection might change slightly as a function of wavelength (λ-direction or X axis on the detector) and position of the fiber in the pseudo-slit (spatial-direction or Y axis on the detector). For most purposes we will adopt an average-sized region of ~4x4 detector pixels in both directions as the MEGARA voxel (see Figure 2).

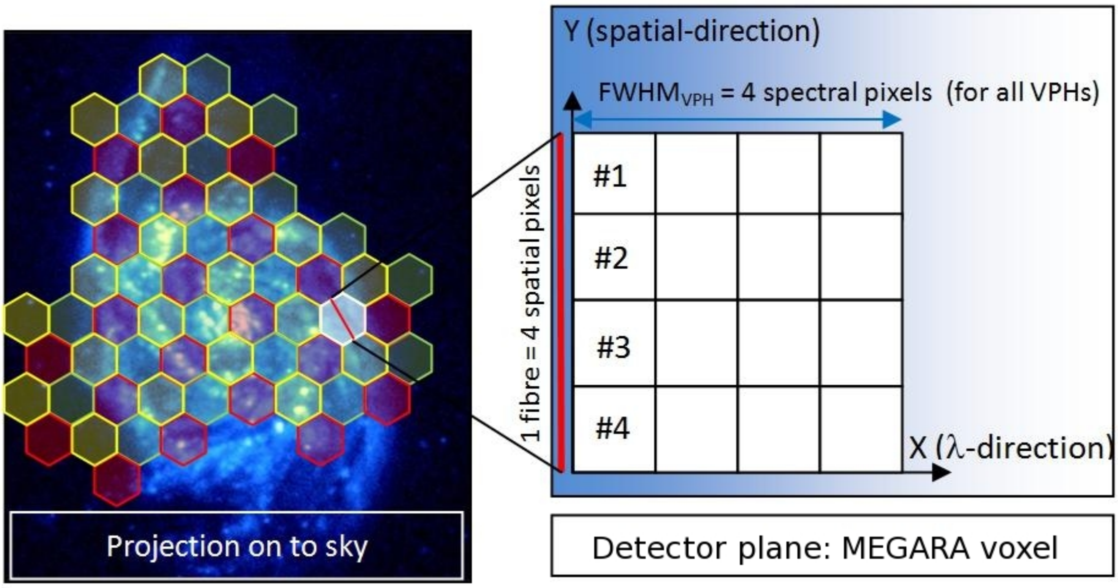


***Figure 2:*** *MEGARA spaxel & voxel. The left panel shows a conceptual representation of the IFU configuration of MEGARA with different hexagonally shaped spaxels in different colors. The right panel shows a schematic projection on the detector of the light coming from the fiber whose corresponding spaxel is marked in white in the left panel.*

## 3.22. Spectral resolution

See §§3.8 and 3.21.

## 3.23. VPH

Volume-Phase Holographic (VPH) gratings diffract light by refractive index modulations within a thin layer of material sandwiched between two glass substrates. Light is diffracted at angles corresponding to the classical grating equation as a function of the incident angle and the frequency of the index modulation at the surface of the grating. The diffraction efficiency, however, is a strong function of the relationship between the angle of incidence and angle of diffraction with respect to the fringes formed by the refractive index modulations within the volume of the grating. If these relationships satisfy the Bragg condition, which also depends on the depth of the grating volume and on the intensity of the grating fringes, then high peak diffraction efficiencies, approaching 100%, are possible [R.19]. For more information, consult [R.20].

The definitive list of MEGARA VPHs and their basic properties (dispersion, spectral range, and spectral resolution) is provided in Table 1 [R.51].

| VPH Name | Setup | $R_{FWHM}$ | $\lambda_1$-$\lambda_2$ Å | λc Å | $\Delta\lambda_{FWHM}$ (@ λc) Å | $\Delta v_{FWHM}$ km/s | line res Å/pix |
|---|---|---|---|---|---|---|---|
| VPH405-LR | LR-U | 6028 | 3653 – 4386 | 4051 | 0.672 | 50 | 0.17 |
| VPH480-LR | LR-B | 6059 | 4332 – 5196 | 4800 | 0.792 | 49 | 0.20 |
| VPH570-LR | LR-V | 6080 | 5143 – 6164 | 5695 | 0.937 | 49 | 0.23 |
| VPH675-LR | LR-R | 6099 | 6094 – 7300 | 6747 | 1.106 | 49 | 0.28 |
| VPH799-LR | LR-I | 6110 | 7220 – 8646 | 7991 | 1.308 | 49 | 0.33 |
| VPH890-LR | LR-Z | 6117 | 8043 - 9630 | 8900 | 1.455 | 49 | 0.36 |
| VPH410-MR | MR-U | 12602 | 3917 - 4277 | 4104 | 0.326 | 24 | 0.08 |
| VPH443-MR | MR-UB | 12370 | 4225 – 4621 | 4431 | 0.358 | 24 | 0.09 |
| VPH481-MR | MR-B | 12178 | 4586 – 5024 | 4814 | 0.395 | 25 | 0.10 |
| VPH521-MR | MR-G | 12035 | 4963 – 5443 | 5213 | 0.433 | 25 | 0.11 |
| VPH567-MR | MR-V | 11916 | 5393 – 5919 | 5667 | 0.476 | 25 | 0.11 |
| VPH617-MR | MR-VR | 11825 | 5869 – 6447 | 6170 | 0.522 | 25 | 0.13 |
| VPH656-MR | MR-R | 11768 | 6241 – 6859 | 6563 | 0.558 | 25 | 0.14 |
| VPH712-MR | MR-RI | 11707 | 6764 – 7437 | 7115 | 0.608 | 26 | 0.15 |
| VPH777-MR | MR-I | 11654 | 7382 – 8120 | 7767 | 0.666 | 26 | 0.17 |
| VPH926-MR | MR-Z | 11638 | 8800 - 9686 | 9262 | 0.796 | 26 | 0.20 |
| VPH665-HR | HR-R | 18700 | 6445 - 6837 | 6646 | 0.355 | 16 | 0.09 |
| VPH863-HR | HR-I | 18701 | 8372 - 8882 | 8634 | 0.462 | 16 | 0.12 |

***Table 1:*** *MEGARA VPHs characteristics for the LCB IFU and MOS modes.*

## 4. SCOPE

This document presents the Users Guide of the MEGARA ETC, which is a software tool included in the MOPSS. It includes user documentation detailing relevant information for users, in particular, the physical models, assumptions, and equations used in the tool.

The UCM group of Extragalactic Astrophysics and Astronomical Instrumentation (GUAIX) is responsible of developing this tool. A first prototype of this tool was presented at the Preliminary Design Phase of the instrument. It has been updated and improved for the Critical

Design Review of MEGARA, accounting for the changes performed to its design.

The MEGARA ETC is a tool intended to simulate the SNRs or limiting fluxes (and magnitudes) that would be obtained for a given exposure time and GTC+MEGARA setup, in both continuum and line emission. A set of input parameters defining the continuum flux distribution and/or the wavelength and FWHM of the line of the input source must be provided, as well as those defining the instrument configuration, atmospheric conditions of the run, and some characteristic of the observational strategy.

## 5. THE ONLINE VERSION

The latest and most current version of the MEGARA ETC (v0.4.2, February 2016) is now accessible online, via any web browser, and from any platform. It does not require any special environment, nor installation. The computation is done on the server where the ETC code is and does not require, any long, any more local resources than to display a webpage. While no installation is necessary, it should be noted that an internet connection is needed for its usage. Moreover, a server downtime would prevent access to the software. For this reason, we have kept the previous stand-alone version (v0.4.1) available for download.

The core code of this online version is the same as the one for the offline version (v0.4.1). It is written in Python-2.6 and uses the libraries numpy[1] and scipy[2]. We make use of the free and open-source Django Python Web Framework[3] (v.1.9). It is one of the most advanced and stable web framework available today, and allows us to set up the required architecture for outputting results generated by Python codes to be displayed in a web browser. Django basically brings the power of Python to the web. For example, we can now easily generate graphical outputs using modules such as matplotlib[4] that produces figures of publication quality. Another advantage of using this framework is for its scalability. New functionalities can be added more easily than the previous standalone versions. Without going in too much details about Django, it is helping to do the following:

- A python code on the server generates the input form fields on top of a HTML/CSS/JS template page, and sends the finalized HTML page (what the user sees).

- The GET method is used to send the user's inputs back to the server. Computations are done on the server, results are generated, and sent back to the HTML page.

It turns out that the user does not need to know any of this since the user will only interact with the ETC via a common HTML form. What should be noted is that we are using the GET method for sending the form's inputs. This method allows the user to save, to bookmark, and to share the computation results with others, since all the inputs appear in the URL.

The current ETC version has been tested on different platforms (web browsers), such as Mac

---

[1] Webpage: http://numpy.scipy.org/

[2] Webpage: http://www.scipy.org/

[3] Webpage: https://www.djangoproject.com/

[4] Webpage: http://matplotlib.org/

OS X (Chrome, Safari, Firefox), iPad (Safari), iPhone (Safari), and Linux (Fedora, Ubuntu, CentOS) (Firefox).

# 6. PHYSICAL CONSIDERATIONS FOR THE MEGARA ETC

The MEGARA ETC considers the transmission curves measured for the atmosphere + telescope + instrument complete system. We comment on them below. We also comment on the source flux spectra considered for the continuum distribution, on how they are normalized to a given input magnitude or flux in a certain photometric band, and on the sky emission spectra assumed in the ETC, according to the night conditions.

## 6.1. Transmission of the telescope

The transmission curve of the telescope in *Figure 3* (grey line) accounts for the transmission of the three aluminum-coated mirrors of GTC.

## 6.2. Transmission of the instrument

In *Figure 3*, we show the transmission curves of MEGARA in the LCB/MOS modes, for low, medium, and high spectral resolution (LR, MR, and HR), as a function of the wavelength [R.52].

The transmission curves in dashed lines include the transmission of the Folded-Cassegrain subsystem + the spectrograph + the grating subsystem in LR, MR, and HR, considering the VPH that covers optimally each wavelength region in each spectral resolution. The transmission curves shown below include the GTC transmission at the top (solid line).

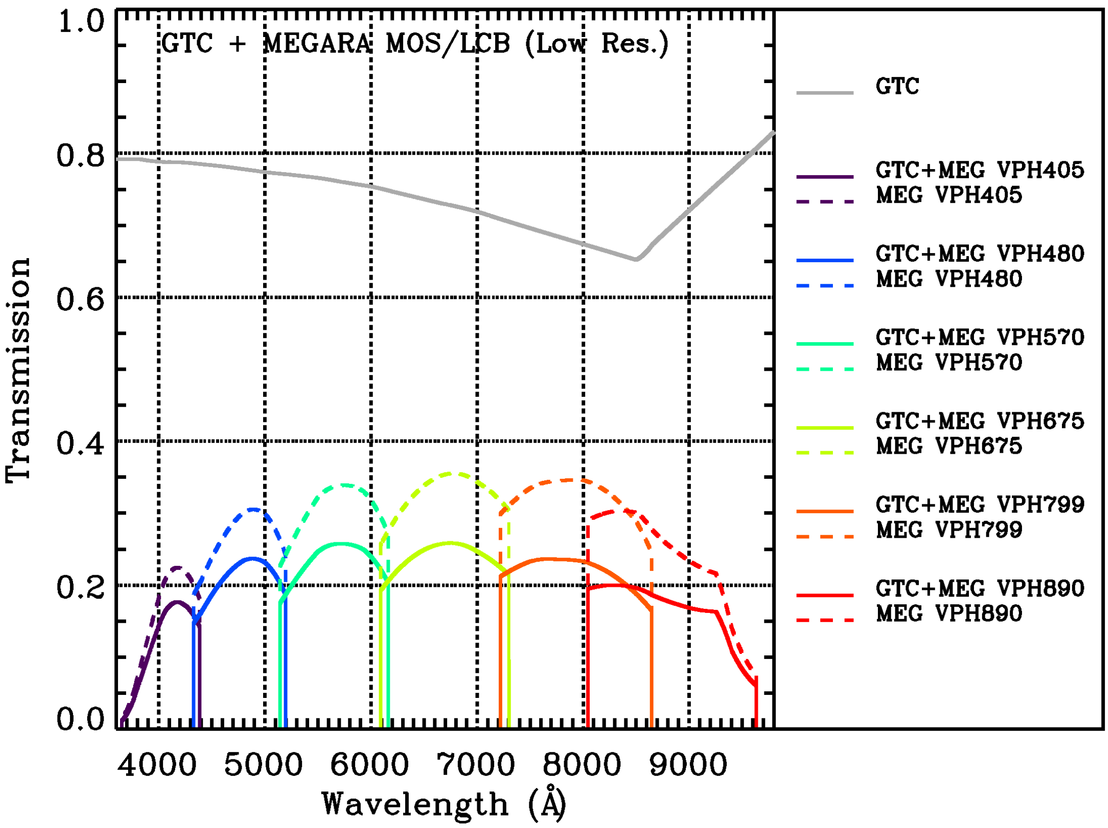
GTC + MEGARA MOS/LCB (Low Res.)
Transmission
Wavelength (Å)
1.0
0.8
0.6
0.4
0.2
0.0
4000
5000
6000
7000
8000
9000
GTC
GTC+MEG VPH405
MEG VPH405
GTC+MEG VPH480
MEG VPH480
GTC+MEG VPH570
MEG VPH570
GTC+MEG VPH675
MEG VPH675
GTC+MEG VPH799
MEG VPH799
GTC+MEG VPH890
MEG VPH890

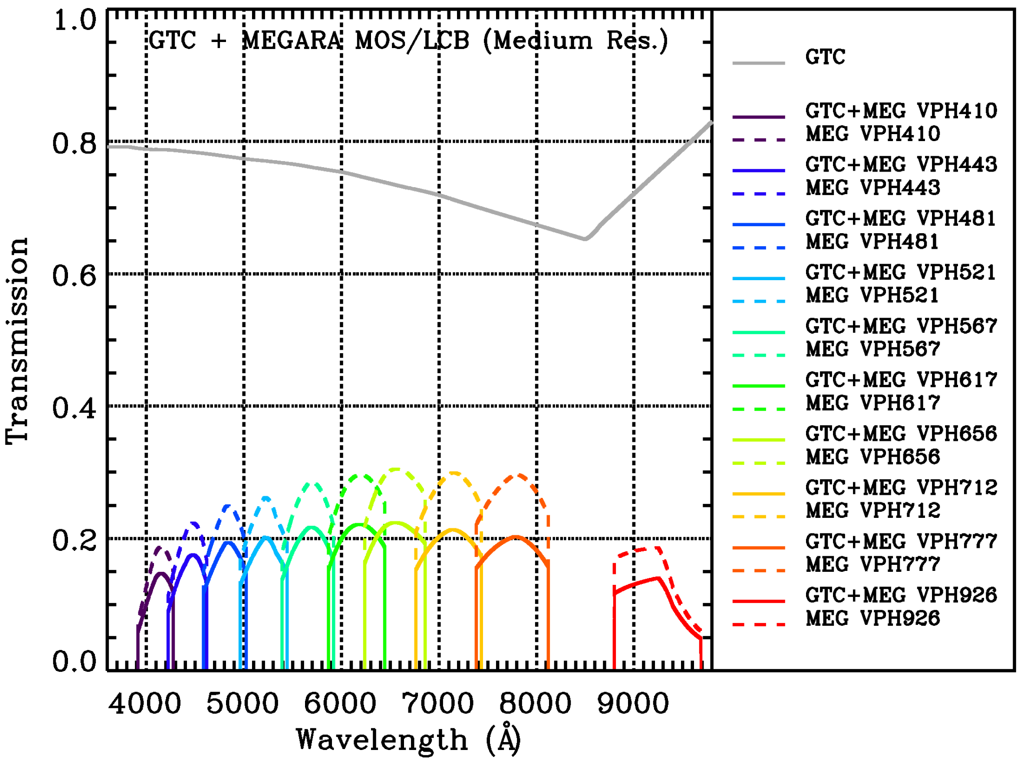
GTC + MEGARA MOS/LCB (Medium Res.)
Transmission
Wavelength (Å)
1.0
0.8
0.6
0.4
0.2
0.0
4000
5000
6000
7000
8000
9000
GTC
GTC+MEG VPH410
MEG VPH410
GTC+MEG VPH443
MEG VPH443
GTC+MEG VPH481
MEG VPH481
GTC+MEG VPH521
MEG VPH521
GTC+MEG VPH567
MEG VPH567
GTC+MEG VPH617
MEG VPH617
GTC+MEG VPH656
MEG VPH656
GTC+MEG VPH712
MEG VPH712
GTC+MEG VPH777
MEG VPH777
GTC+MEG VPH926
MEG VPH926

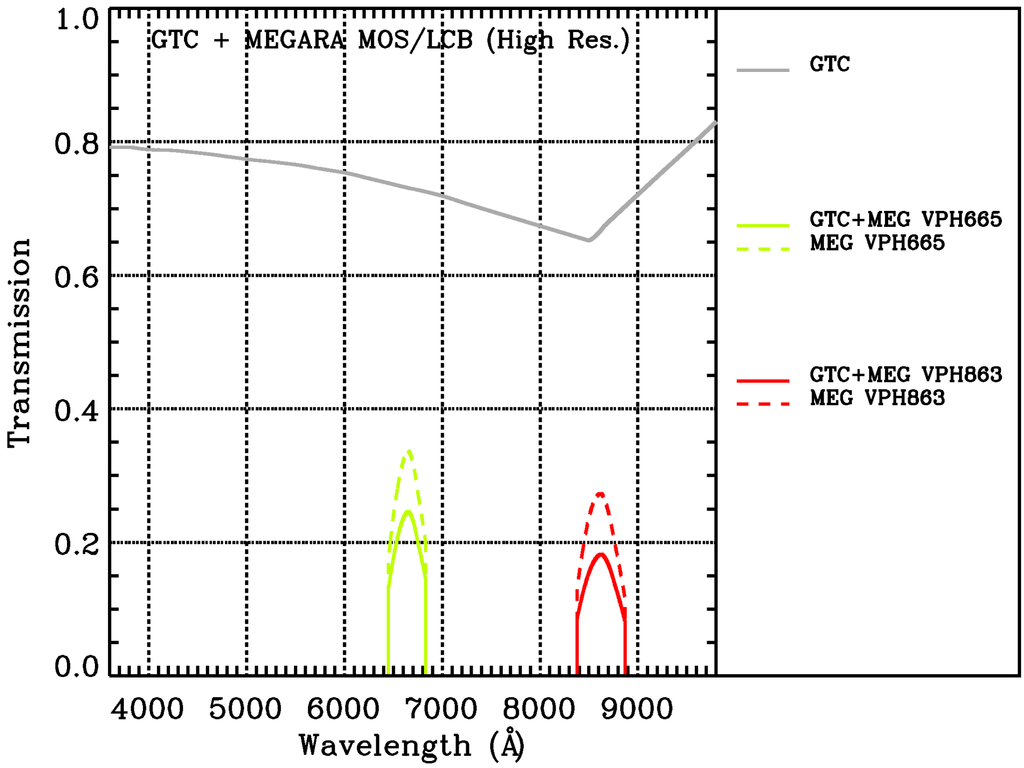


***Figure 3:*** *Transmission curves of GTC+MEGARA (continium lines) and MEGARA (dashed lines) in the LCB/MOS modes, for low, medium, and high spectral resolution as a function of the wavelength.*

### 6.2.1. Folded-Cassegrain Subsystem

The curve of the Folded-Cassegrain subsystem includes the effects in transmission efficiency of the field lens + microlens + pupil system (for LCB/MOS modes) + Focal Ratio Degradation (FRD) + fiber transmission (considering a length of the fiber link of 40 m) + the fiber exit [R.52]. All these curves are represented in Figure 4.

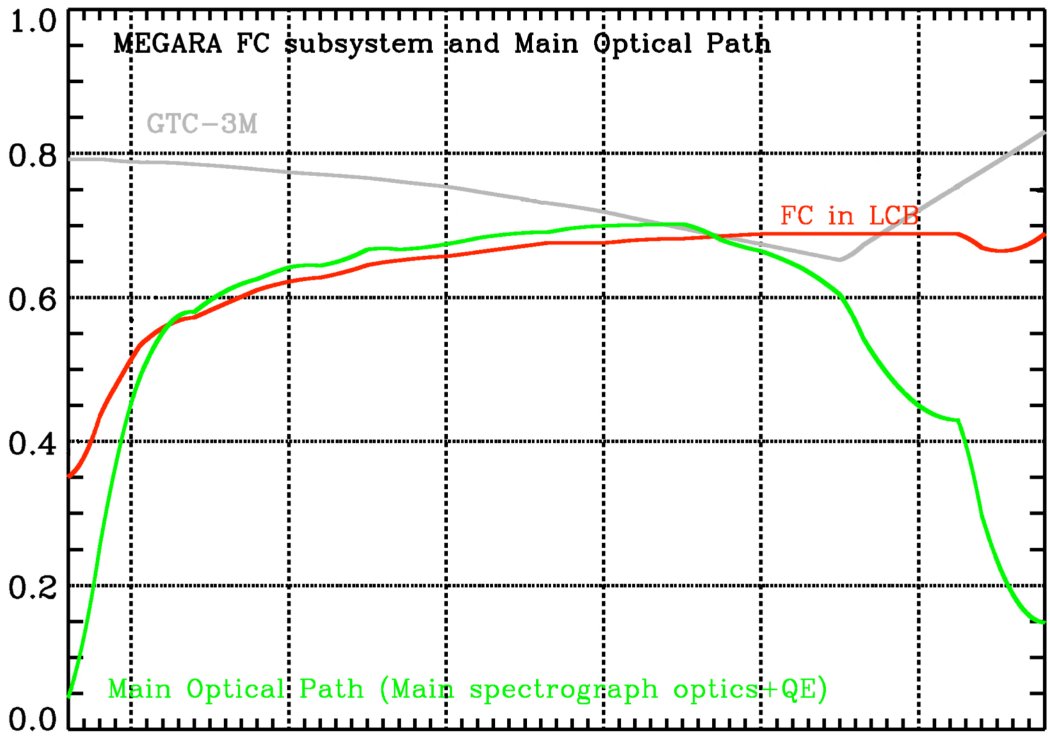


***Figure 4*** *: Transmission curves of the MEGARA Folded-Cassegrain subsystem and of the Spectrograph subsystem including the main optics of the spectrograph and the detector QE (but no grating).*

The attenuation power of the MEGARA fibers, α(λ), is plotted in *Figure 5*. The final attenuation of a fiber depends on its length ($L_{fiber}$), according to:

$$A_{\rm fibre}(\lambda) = \alpha(\lambda) \cdot L_{\rm fibre} \quad . (2)$$

If α(λ) is provided in dB/km (as in *Figure 5*), the length of the fiber must be provided in km. Finally, the total transmission of the fiber can be estimated as follows:

$$T_{\rm fibre}(\lambda) = 10^{[A_{\rm fibre}(\lambda)/(-10)]} \quad . (3)$$

An average fiber length of $L_{fiber}$ = 40 m has been assumed for MEGARA, obtaining the fiber transmission curve represented in Figure 4.

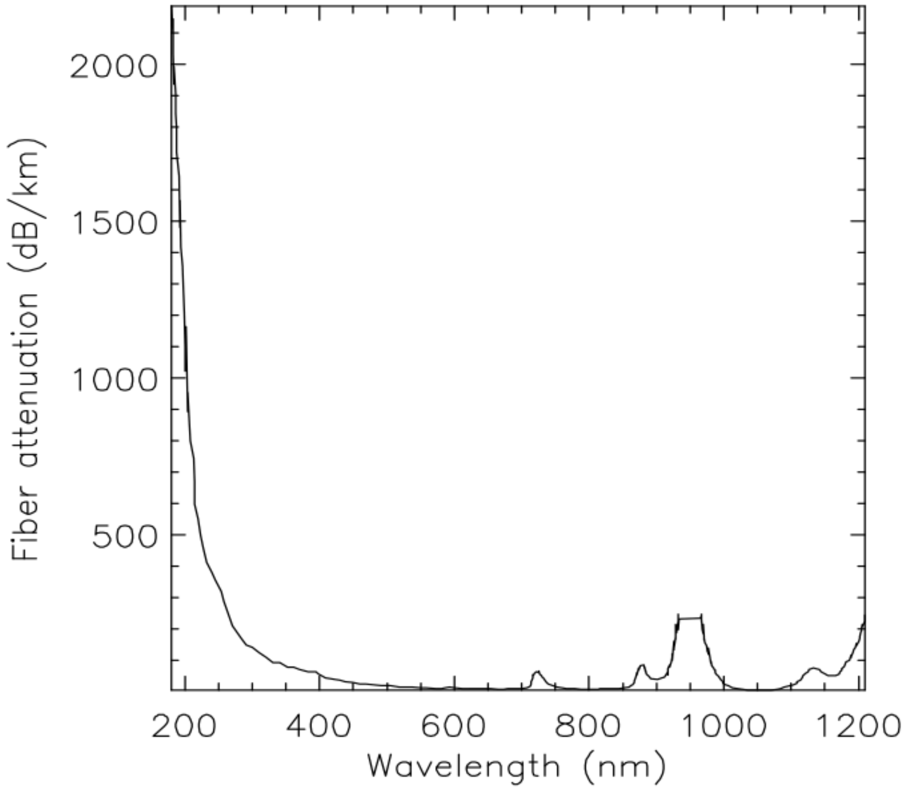


***Figure 5:*** *Attenuation power of MEGARA fibers.*

### 6.2.2. Spectrograph Subsystem

The transmission curve of the spectrograph accounts for the transmission of the main spectrograph optics (entrance window + lenses + mirrors) + the detector QE [R.52]. See Figure 4.

The detector will be an E2V CCD231-84-0-E74 device [R.51]. This measures 4096 x 4112 x 15μm pixels and has four outputs. There are several variants of this device but MEGARA will use the Deep-Depletion Silicon version with the Astro Multi-2 AR coating as being the one best suited for the demands of MEGARA. The CCD has excellent QE across almost the whole visible spectrum.

The ETC requires the read-out noise (RON) in electron per pixel (< 3 electrons, see §3.18) and the dark current noise (DC) in electron per pixel and per second. The last one is negligible for MEGARA detector (0.02 electrons/pixel/hour) [R.52].

### 6.2.3. Grating Subsystem

The grating subsystem accounts for the transmission of the different VPHs + the efficiency of associated elements (including the order sorting filter to be used in the VPHs transmitting in the red part of the optical spectrum). The VPHs transmission curves are plotted in Figure 6, including the efficiency of adjacent elements in LR, MR, and HR (as the prism in the MR and HR gratings and the vigneting due to the HR prism [R.52]).

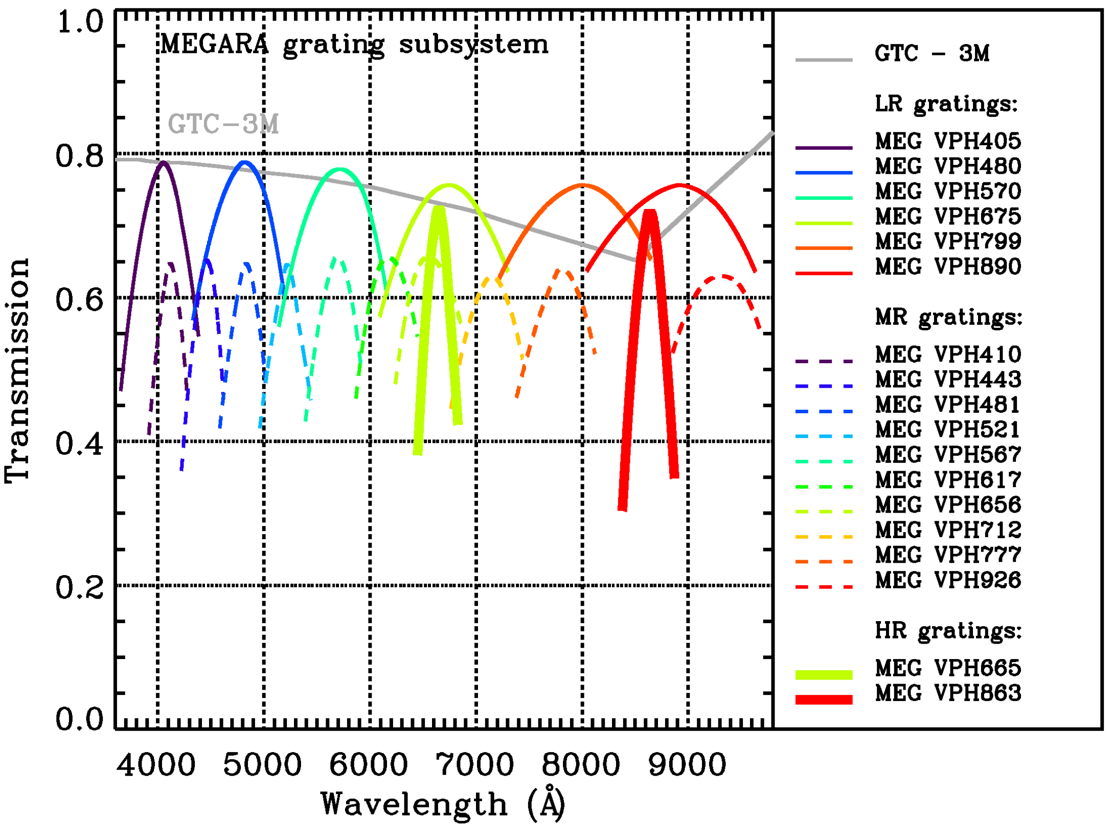


***Figure 6****: Transmission curves of the different MEGARA grating subsystem, including the efficiency of associated elements and order sorting filters when needed.*

## 6.3. Source flux spectra

In the ETC, the input total Vega magnitude of the source continuum in any given input photometric band is converted into total flux in that band ($F_i$), according to [R.23]:

$$F_i = F_{0,i} \cdot 10^{-(m_i - m_{0,i})/2.5}, \quad (4)$$

where $F_{0,i}$ and $m_{0,i}$ are the Vega flux and magnitudes in that band, and $m_i$ is the target magnitude in that band. The magnitudes and fluxes of Vega in different bands are provided in *Table 2*, as well as the central wavelengths $\lambda_{0,i}$ and bandwidths $\Delta\lambda_{0,i}$ of the considered Johnson-Bessel bands.

| Band | Vega magnitude $m_0$ | Vega flux @$\lambda_0$ $F(\lambda_0)$ (erg/s/cm2/Å) | Eff. wavelength $\lambda_0$ (Å) | Band-width $\Delta\lambda_0$ (Å) |
|---|---|---|---|---|
| U Johnson-Bessel | 0.030 | 4.22E-9 | 3657.5 | 577 |
| B Johnson-Bessel | 0.035 | 6.20E-9 | 4334.5 | 975 |
| V Johnson-Bessel | 0.035 | 3.55E-9 | 5374.0 | 846 |
| R Johnson-Bessel | 0.075 | 1.795E-9 | 6272.5 | 1273 |
| I Johnson-Bessel | 0.095 | 8.60E-9 | 8722.0 | 2980 |

***Table 2:*** *Vega magnitudes and fluxes in certain Johnson-Bessel photometric bands [R.31]. Central wavelengths and bandwidths of the Johnson-Bessel photometric filters [R.32-R.34].*

The flux computed above corresponds to the flux at the effective wavelength of the corresponding band (see column 4 of *Table 2*). Note that this flux is given per Å, by definition.

The input source spectrum template $F_{template}(\lambda)$ selected by the user is normalized in order to have a flux per Å at the effective wavelength of the input continuum band equal to unity:

$$\mathcal{F}_{\text{norm}}(\lambda) = \frac{\mathcal{F}_{\text{template}}(\lambda)}{\int_{\lambda_{0,\text{i}}-0.5\mathring{\text{A}}}^{\lambda_{0,\text{i}}+0.5\mathring{\text{A}}} \mathcal{F}_{\text{template}}(\lambda) \cdot T_i(\lambda) \cdot d\lambda}$$

, (5)

where $T_i(\lambda)$ represents the transmission of the considered band (see *Figure 7*). The normalized spectrum is then scaled to ensure that the flux per Å in the input continuum band at the effective wavelength equals to the input flux per Å provided by the user in that band, as follows:

$$\mathcal{F}_{\text{scaled}}(\lambda) = F(\lambda_{0,\text{i}}) \cdot \mathcal{F}_{\text{norm}}(\lambda)$$

, (6)

where $F_{norm}(\lambda)$ is obtained through eq. 5. Notice that $F_{scaled}(\lambda)$ at the effective wavelength of the input continuum band *i* is the one inserted by the user as input:

$$\int_{\lambda_{0,\text{i}}-0.5\mathring{\text{A}}}^{\lambda_{0,\text{i}}+0.5\mathring{\text{A}}} \mathcal{F}_{\text{scaled}}(\lambda) \cdot T_i(\lambda) \cdot d\lambda = F(\lambda_{0,\text{i}})$$

. (7)

$F_{scaled}(\lambda)$ represents the energy flux spectrum of the input source, as set by the user's inputs. If the input source is punctual (as in some cases of the ETC if a stellar spectrum is selected as input), this energy flux spectrum corresponds to the emission in the whole source area (i.e., it is given in erg/s/cm$^2$/Å); whereas if the input source is extended (rest of cases in the ETC), it corresponds to the energy flux spectrum of the source per arcsec$^2$ (as the input continuum magnitude or flux provided by the user is requested to be given per arcsec$^2$, see §7.2).

The total continuum flux of the input source can be easily computed at any other photometric band *j*, as follows:

$$F_{\mathrm{j}} = \int_{\lambda_{j,0}-\Delta\lambda_j/2}^{\lambda_{j,0}+\Delta\lambda_j/2} \mathcal{F}_{\mathrm{scaled}}(\lambda) \cdot T_j(\lambda) \cdot d\lambda \quad . (8)$$

$T_j(\lambda)$, $\lambda_{j,0}$, and $\Delta\lambda_j$ being the transmission curve, central wavelength, and the bandwidth of the photometric band *j*.

The template spectra of the MEGARA ETC ($F_{template}(\lambda)$ in Eq. 5 above) are the same as those in the ETC of GTC/Elmer instrument, kindly made available by M. García-Vargas. It consists of a set of standard spectra of stellar, galactic, and extra-galactic objects. They are plotted in Figures 8 and 9.

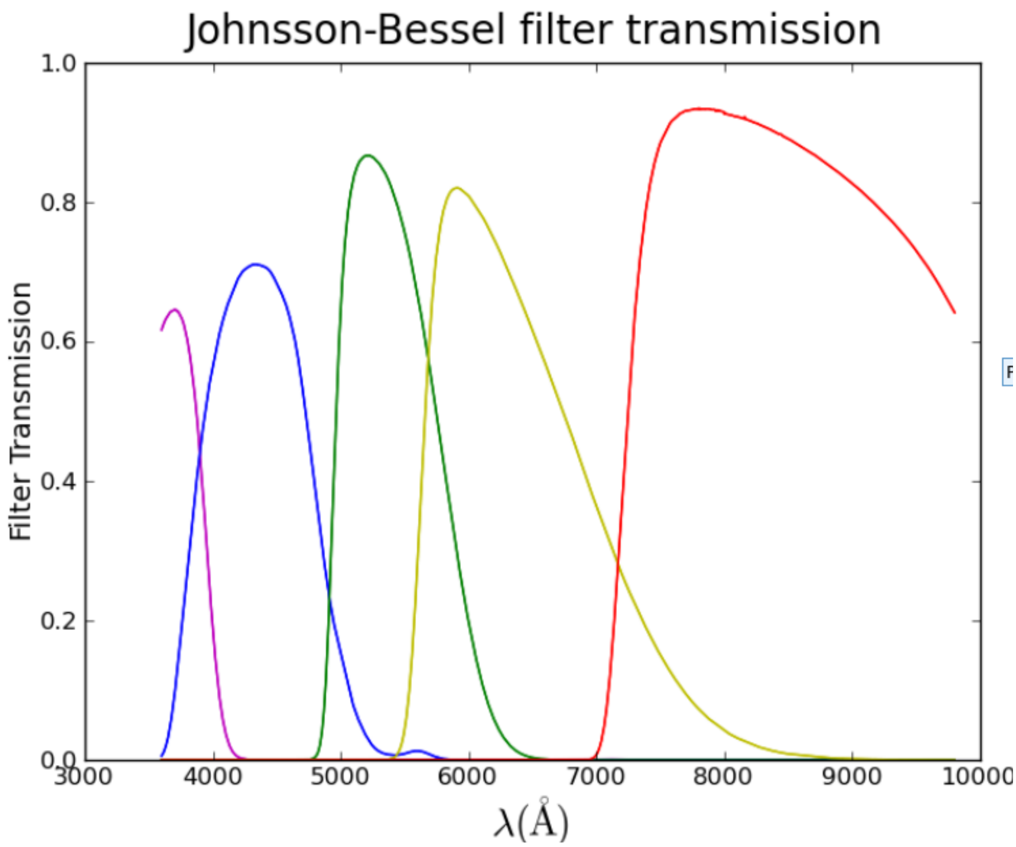


***Figure 7:*** *Transmission curves of the Johnson-Bessel photometric bands [R.35]. All transmission curves of MEGARA ETC are provided in steps of 0.1Å, obtained through linear interpolation.*

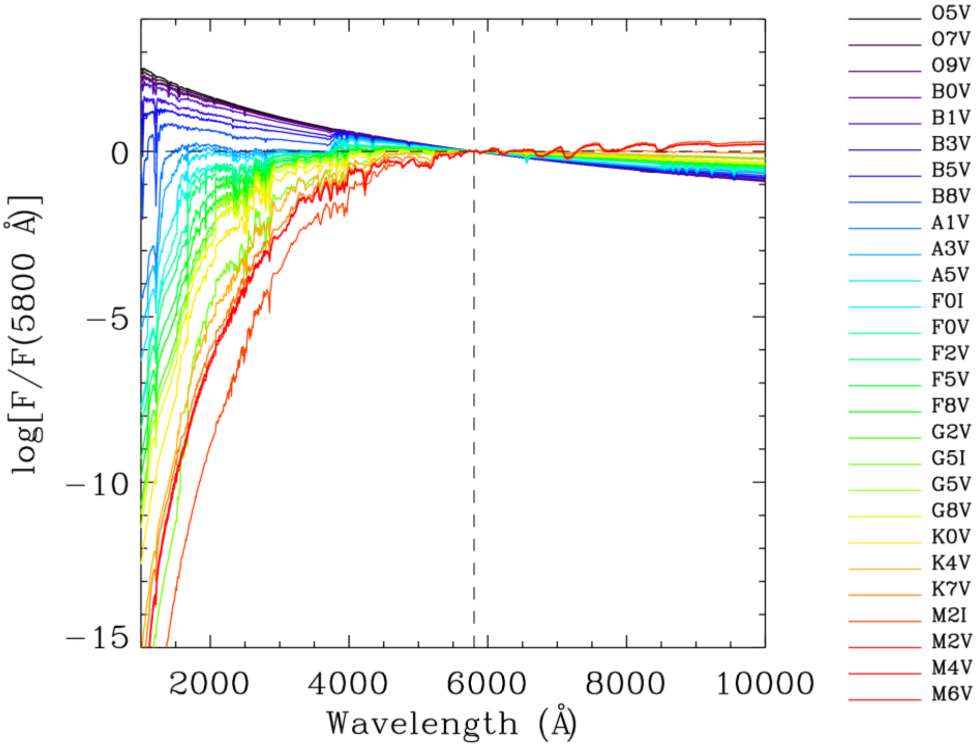


***Figure 8:*** *Input spectra of typical stellar types available in the MEGARA ETC.*

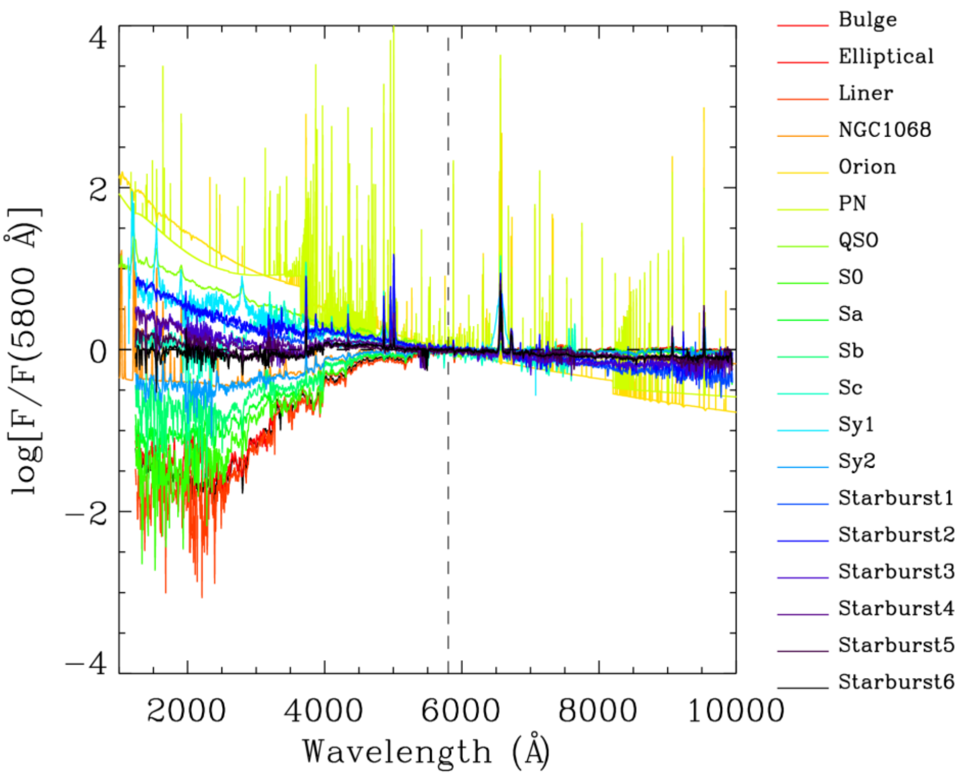


***Figure 9****: Input spectra of typical Galactic and Extragalactic targets available in the MEGARA ETC.*

## 6.4. Sky background emission

The present version assumes that the input sky spectrum in the optical range is uniform. The sky emission magnitude is initially set in the photometric band that presents a higher overlapping with the wavelength range of the user-selected input VPH (see *Table 1*). This magnitude (provided by arcsec$^2$, consult *Table 2*) is converted to flux per Å using Eq. 4. The sky emission in any band can be then estimated with Eq. 8. As the sky emission in El Roque de los Muchachos Observatory Observatory has found to be quite similar to that of Mauna Kea [R.36], a sky spectrum of Mauna Kea will be used for GTC/MEGARA.

## 6.5. Atmospheric transmission and extinction

The atmospheric extinction on La Palma is discussed in detail in [R.53]. It is possible to separate the extinction into two components: one due to Rayleigh scattering by air molecules and absorption by ozone (which is wavelenght-dependent), and another due to dust (aerosol) scattering (which in independent on wavelength).

The wavelength-dependent component measures the atmospheric transmission in a dust-free atmosphere. This component at El Roque de los Muchachos Observatory is quite similar to that of the Mauna Kea observatory in the optical range, although slightly lower [R.36, R.37]. In *Table 3*, we show a comparison of the atmospheric transmission of both sites. The atmospheric transmission curve of Mauna Kea in the optical range is plotted in *Figure 10* (red line).

The (dust-free) atmospheric transmission curve available for Mauna Kea does not account for a series of atmospheric absorption features usually present in observing sites, as those present in the atmospheric transmission curve of the AAO site (see blue line in *Figure 10*). In order to account for the global transmission curve of La Palma and to also include these absorption features, we have combined both curves to obtain a combined transmission curve representative of the atmospheric transmission in La Palma for the MEGARA ETC (black line in *Figure 10*).

Dust scattering at the Roque de los Muchachos observatory does not depend strongly on wavelength over the optical range [R.53]. Therefore, it just includes a constant to the wavelength-dependent term of the atmospheric extinction (in units of mag per airmass). The extinction due to dust scattering varies from night to night, but is usually less than a few tenths of a magnitude per unit airmass. We do not account for the atmospheric extinction by dust (the wavelength-independent term) in the MEGARA ETC.

| **Wavelength (Å)** | **Atm. transmission (%) @La Palma** | **Atm. transmission (%) @Mauna Kea** |
|---|---|---|
| 4000 | 72 | 79 |
| 4500 | 80 | 85 |
| 5000 | 84 | 89 |

***Table 3:*** *Comparison of the atmospheric transmission of La Palma and Mauna Kea observatories [R.36, R.37].*

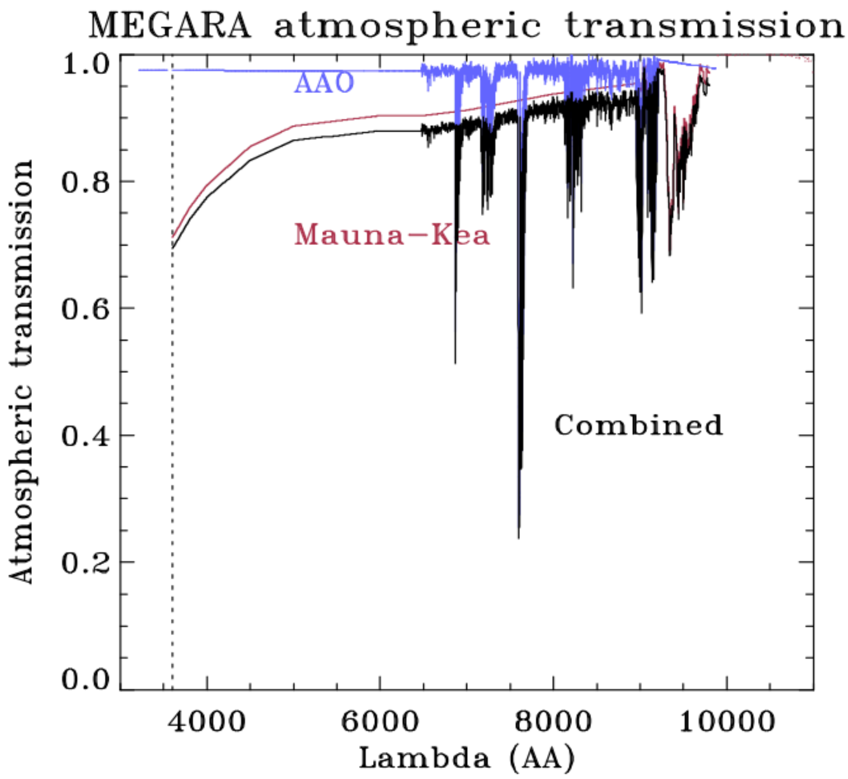


*Figure 10: Transmission curve of the atmosphere used in MEGARA ETC.* ***Blue curve****: Empirical atmospheric transmission curve from the Anglo-Australian Observatory (AAO), used in the OSIRIS ETC [R.38].* ***Red curve****: Atmospheric transmission curve from Mauna-Kea observatory [R.36].* ***Black curve****: Combined AAO-Mauna-Kea atmospheric transmission curve, finally used in MEGARA ETC.*

## 7. THE MEGARA ONLINE EXPOSURE TIME CALCULATOR

The actual version of the MEGARA ETC provides estimates of the SNRs on continuum and line flux distributions that would be obtained for a given exposure time, GTC+MEGARA setup, and certain observing conditions, according to the current MEGARA design [R.51]. Future versions shall estimate the limiting flux achieved for a given exposure time in both continuum and line cases, and derive the required exposure time for achieving a given SNR at the central wavelength of a VPH in the case of the continuum or at a given wavelength in the case of an emission line.

The current version can be used to derive the computations above just using an iterative method (changing the input magnitude/flux and the exposure time) until the required SNR is obtained in the central wavelength of the VPH for continuum or at the line. Now, the tool provides the SNR at the central wavelength of the VPH when considering a voxel in continuum estimates.

## 7.1. Graphical User Interface

This version of the MEGARA ETC allows the user to select the input parameters in a web form via a single web browser page. Output estimates on the SNRs are shown in the bottom half of the page, and can be saved into a text file. As of this version, graphical outputs are also generated, bringing the need to save the graphical results as well. One of the advantage of having the ETC in a web browser is that saving graphics from a browser has nowaday become an easy task with most common browsers. We have thus provided a way to show the results in a separate window (by clicking on the "**New Window**" button), where the user will be able to print/save in any format the browser that is in use permits. In Figure 11, we show a snapshot of the graphical user interface (GUI) of the online version of the ETC tool (v0.4.2, February 2016).

Future versions of the MEGARA ETC will provide other output predictions that could be useful to the observer required exposure times to get certain SNRs, the addition of input line on the continuum, etc. Additional buttons for choosing these sort of required outputs and graphical windows will be added to this preliminary tool.

Once the user has selected a certain combination of input parameters, he/she can start the SNR estimate by clicking the "**Submit**" button. The input parameters will be updated in the "Input parameters" output window, and the resulting SNRs will appear in the "Continuum output SNR" and "Line output SNR" columns in the "Results" section at the bottom half of the MEGARA ETC, for the selected continuum and the line input parameters respectively.

Results can either be downloaded as a plain text file (.txt) by clicking on the "**Print to file**" button, or opened in a new window by clicking on the "**New Window**" button. The text file will be downloaded, in general, in the browser's Download directory.

The input fields can be reset to its default values by clicking on the "**Reset**" button.

For more information, the user can click on the "**Help**" button of the MEGARA ETC. Many input fields have an appended tab marked as "**?**" that provides a quick help to the content of the field.

To quit the ETC, just close the browser window.

The tool has several warnings implemented to avoid incorrect input or unreallistic input physical values. When the "Submit" button is pressed, errors messages and input suggestions are shown in the "**Results**" window to inform the user of a problem.

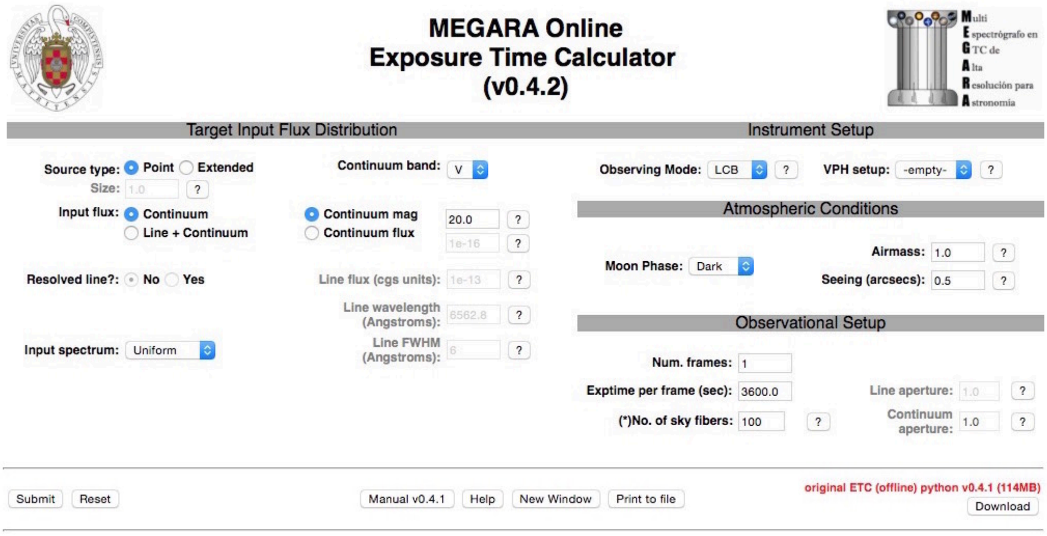


***Figure 11:*** *GUI of the online version of MEGARA ETC (v0.4.2, February 2016). The form may appear slightly different from one browser to another and from one operating system to another.*

## 7.2. Input parameters

The GUI of the ETC allows the user to fix a set of input parameters describing the characteristics of the observation they are interested in simulating, specifically those concerning to:

- the input target (geometry, spectrum, magnitude of continuum/line, FWHM and wavelength of line),
- the observing night (moon phase, seeing, airmass),
- the observing run characteristics (number of frames, exposure time per frame, number of sky mini-bundles used, spectral apertures to get continuum and line fluxes),
- the instrumental setup (VPH of use, quantum efficiency of the CCD+coating of use).

The following parameters are fixed internally in the software and concern to the GTC+MEGARA specifications:

- the telescope (mirrors transmission, collecting area, see §6.2),
- the transmission of MEGARA (Folded-Cassegrain + spectrograph + grating transmission, see §6.2),
- detector plate scale.

The input parameters that can be modified by the user are detailed below.

### 7.2.1. <u>User required outputs</u>

The user must select the kind of output provided by the ETC. Each kind of output requires certain different input parameters. For a given input instrumental setup and atmospheric conditions, the user can request:

1. The SNR expected by the ETC on a given input source for a given input exposure time, both on a continuum or in a line flux distribution.

2. The SNR vs. wavelength expected by the ETC on a given input source for a given input exposure time, in continuum flux distributions.

3. The exposure time required to achieve a given SNR at the central wavelength of the selected VPH for the input source in continuum or at a given emission line.

4. The limiting magnitude or flux of a continuum or line flux distributions for a fixed SNR achieved for a given exposure time.

The computations available in the current online version are the first two. However, computations 3 and 4 can be estimated by iteratively changing the input flux and/or exposure time until the desired SNR is provided as output in the resolution element that the user is considering (detector pixel, voxel, spaxel, or total source).

In the two former cases, the field indicating an input exposure time is mandatory (the SNR estimate is the output), whereas in the two last ones, the field indicating the input SNR to achieve is mandatory (being the exposure time the output).

#### 7.2.2. Target Input Flux Distribution

This set of parameters is intended to describe the flux distribution of the source to be observed.

1. **Target type:** It indicates if the source is unresolved (point source) or extended. If a point source is chosen, the target object is assumed to be an emitter with negligible intrinsic angular size. This can be selected for objects with an angular radius much smaller than the seeing-disk size. If extended source is chosen, the target object is assumed to have a uniform intensity across its whole projected area. If “Source_type=extended”, then the input parameter "Size" becomes mandatory.

2. **Target projected size:** For extended sources, apparent projected area of source in arcsec$^2$ ($A_{obj}$). Circular shape is assumed for the source. This parameter is available only if the 'Source Type=Extended' option is set.

3. **Input target flux:** Type of data inserted to get the SNR. If "Input flux=Continuum", only input data necessary to define the continuum of the source are required for computation. If "Input flux=Line+Continuum", the following input parameters become mandatory too: "Resolved line", "Line flux", "Line wavelength", "Line aperture", and "Continuum aperture".

4. **Resolved line:** This parameter indicates if the line can be resolved or not, and it is relevant only if "Input flux=Line+Continuum". If the line is resolved, the user must insert the line FWHM. Otherwise, the FWHM of the line is determined in the basis of the VPH selected.

5. **Input spectrum:** The target model can be defined by the target spectral type. It uses a

template spectrum, which is scaled to the magnitude and filter provided. The spectral type is used to make the color correction and continuum background subtraction. We remark that no line diagnostics are derived from an input spectrum template, only continuum ones.

6. **Continuum band:** Photometric band in which the input continuum magnitude or flux is provided. The input template spectrum is scaled to the input magnitude in this band.

7. **Continuum magnitude:** For point sources, Vega apparent magnitude of the source continuum in the selected continuum band. For extended sources, the magnitude must be provided per arcsec$^2$ in the selected band. Only available if 'Continuum flux' option is not set.

   Note: This option can be filled if the output requested by the user is an exposure time or a SNR to be determined over the continuum (§7.2.1). It cannot be filled if the users request the estimate of the limiting magnitude over a given continuum template to be achieved in a given exposure time and for a given SNR (§7.2.1). In the current tool, only SNR estimates are provided as outputs, so this option can be filled always, unless 'Continuum flux' option is set.

8. **Continuum flux:** For point sources, flux of source continuum in c.g.s. units (erg/s/cm$^2$/Å) in the selected continuum band. For extended sources, this flux is provided per arcsec$^2$. Only available if the 'Continuum Magnitude' option is not set.

   Note: In the current prototype, this input can be filled in any case, but in future versions of the tool this input shall be blocked if it requested as an output (§7.2.1).

9. **Line flux:** For point sources, flux of line in c.g.s. units (erg/s/cm$^2$). For extended sources, this flux must be provided per arcsec$^2$. This parameter is available only if the 'Input flux=Continuum+Line' option is set.

   Note: This input shall be blocked in future versions of the tool that may provide it as output (§7.2.1).

10. **Line wavelength:** Line wavelength in Å. This parameter is available only if the 'Input flux = Continuum+Line' option is set.

11. **Line FWHM:** Line FWHM in Å. If the line is not resolved, the nominal FWHM of the selected VPH at its central wavelength is assumed (consult Table 1). This parameter is available only if the 'Input flux=Continuum+Line' and 'Resolved line=yes' options are set.

#### 7.2.3. Instrumental setup

This set of parameters is intended to describe the instrument initial setup (basically, the VPH to be selected by the user).

1. **OM:** In MEGARA, there will be several scientific OMs (see [R.15]). "IFU-only observation" will include: LCB IFU and LCB fast mapping scientific observing modes. "Robotic positioners-only observation" will include the Fiber MOS scientific observing

mode. As indicated above, the LCB IFU and LCB IFU fast mapping OMs will include some fibers from the RPs into the pseudo-slit (56, from 8 positioners) to be used as sky spectra. In the case of Fiber MOS OM the user needs to select some RPs to be devoted to blank-sky measurements.

In general, the number of sky fibers should be defined by the user in the GUI. The LCB mode uses 56 sky fibers by default (as commented above), but this number can be changed.

2. **VPH setup:** The characteristics of each spectral VPH setup are listed in *Table 1*. The wavelength of the input spectral line (in the case that the users require line diagnostics) must be located into the wavelength range of the selected VPH. A program warning is shown if this requirement is not fulfilled and no computation is performed.

### 7.2.4. Atmospheric conditions during the observing run

Depending on the atmospheric conditions during the data taking, the number of photons and the seeing FWHM of the observed source change. The ETC must have these effects into account.

1. **Moon phase:** The following options for the night brightness are available: dark/grey/bright. The sky magnitude at a dark night in La Palma at the zenith is initially set in the photometric band nearest to the user-selected VPH (consult Table 4). These values have been found to be independent of atmospheric extinction, and do not vary appreciably during the night, but with solar cycle, latitude and airmass [R.24]. In the present version, the sky spectrum is assumed to be uniform. In future versions, a typical atmospheric spectrum will be scaled to the selected magnitude [R.21]. The typical average extra brightness between a dark and grey or bright night is added, depending on the user-selected moon phase (consult Table 5), assuming that the difference of emission between dark and bright or dark and grey does not depend on the optical band. The average emission due to zodiacal light, airglow, and starlight has been also considered [R.25].

2. **Airmass:** Airmass scales the number of photons from the sky background according to the following expression [R.26]:

$$S_{\rm sky}(X) = S_{\rm sky}(X=1)\cdot[-0.000278719X^3 - 0.0653841X^2 + 1.11979X - 0.0552132] \quad . (9)$$

3. **Seeing:** FWHM of the seeing in arcsec. The value refers to the FWHM of the seeing disk in V band, at the requested airmass. Note that the variation of seeing with airmass X can be assumed to scale as follows [R.26]:

$$\mathrm{FWHM_{seeing}}(X) = \mathrm{FWHM_{seeing}}(X=1)\cdot X^{3/5} \quad . (10)$$

The above expression can be used to predict the expected seeing at different airmasses, which is some situations can be useful in the case the user needs to simulate observations performed at different telescope elevations. It is important to highlight that the ETC will always assume the user has properly introduced the expected seeing at the quoted airmass.

The seeing value at the selected airmass is written to the "Input parameters" output window of the "Results" menu each time the ETC is executed.

| Band | Sky brightness (mag/arcsec$^2$) | $\gamma$ (photons/s/m/arcsec$^2$/Å) |
|---|---|---|
| U | 22.0 | 0.012 |
| B | 22.7 | 0.012 |
| V | 21.9 | 0.017 |
| R | 21.0 | 0.029 |
| I | 20.0 | 0.049 |

***Table 4:*** *Near-zenith dark-of-moon broad-band sky brightness at La Palma for different bands. Values taken from [R.24].*

| Moon Phase[1] | $\Delta$mag (mag/arcsec$^2$) |
|---|---|
| Bright | 3.1 |
| Grey | 1.5 |
| Dark | 0.5 |

*[1] These values already account for zodiacal light, airglow, and starlight*

***Table 5:*** *V-band extra magnitudes to be added to reference values of sky emission in Table 4, for bright, grey, and dark nights in La Palma [R.25].*

### 7.2.5. Observational Setup

This parameter set describes the characteristics of the observation to be done with MEGARA:

1. **Num. frames:** Number of frames (integer).

2. **Exptime per frame:** Exposure time per frame in seconds. The total exposure time will then be the product of "Num. frames" and the "Exptime per frame" values.

   This exposure time does not take into account instrument and telescope overheads (typically, 20-30% of the required exposure time; consult observing overheads section in GTC web page http://www.gtc.iac.es/observing/). If sky exposures are planned to be required in an observation in order to subtract sky emission, the user must also consider that the total exposure time required for that target could be up to twice the ETC estimates (plus overheads).

   Note: This field can be filled only if the user has not required an exposure time estimate as output (§7.2.1).

3. **SNR:** Input SNR in the case the user is interested in estimating the exposure time to be

used for achieving it. This option is not implemented in the current prototype of the online ETC yet.

Note: In future versions of the tool, this field can be filled only if the user has required the exposure time to achieve a given input SNR as output (§7.2.1).

4. **No. of sky fibers:** Number of sky fibers used to derive the sky spectrum to subtract. If the user has selected the Fiber MOS OM (§7.2.3), the maximum number of fibres is 644, as each actuator has a 7-fibers mini-bundle and there are 92 actuators projected in the pseudo-slit corresponding to this OM [R.51]. In the case of the LCB IFU and LCB IFU fast mapping OMs there are 8 fixed RPs devoted to sky background measurements that will be included into the pseudo-slit of these OMs. Anyway, although 56 is the default value in this case, this number can be modified up to 623 if the user considers that he/she will take sky frames with the same exposure time (567 fibers from the IFU + 56 from the 8 RPs, [R.51]).

5. **Line aperture:** Aperture to derive line flux in spectrum, in line FWHM units ($n_{line}$). This parameter is available only if the 'Input flux=Continuum+Line' option is set.

6. **Continuum aperture:** Aperture to estimate continuum around the line for continuum-subtraction, in line FWHM units ($n_{CS}$). This parameter is available only if the 'Input flux=Continuum+Line' option is set.

## 7.3. Outputs

A summary of the outputs of the ETC is provided here, with some warnings and extra information about the input source flux distribution. Since the current version to-date only provides SNR estimates, we have exclusively detailed them (§7.2.1). We remind the user that the current tool can be used to determine exposure times and limiting fluxes in both continuum and line distributions just using the tool iteratively, changing the input values of flux and/or exposure time until the required SNR on continuum or line is provided as output.

### 7.3.1. Continuum output SNRs

The present version of the ETC provides the SNRs of the continuum input flux distribution expected for a given input parameters set for both, a single frame exposure and for the total number of frames N (SNR of a single frame multiplied by $\sqrt{N}$).

In case we are dealing with a point source, the provided SNRs are for:

- in one fiber: per detector pixel, per spectral pixel, per spectral FWHM, and per Å;
- in the total source area[5]: per spectral pixel, per spectral FWHM, and per Å;

In case of extended sources, the following additional outputs are provided:

- for 1 seeing: per spectral FWHM, per Å, and per spaxel.
- for 1 arcsec$^2$: per spectral FWHM, per Å, and per spaxel.

[5] The number of fibers required to sample the whole source is also provided.

Future improvements to the ETC shall provide the exposure time required to get a given input SNR at the central wavelength of the selected VPH, for a certain set of input parameters. Limiting flux estimates in continuum will also be provided in future versions of the tool.

All these outputs will be provided considering the different spatial and spectral resolution elements on the detector listed above.

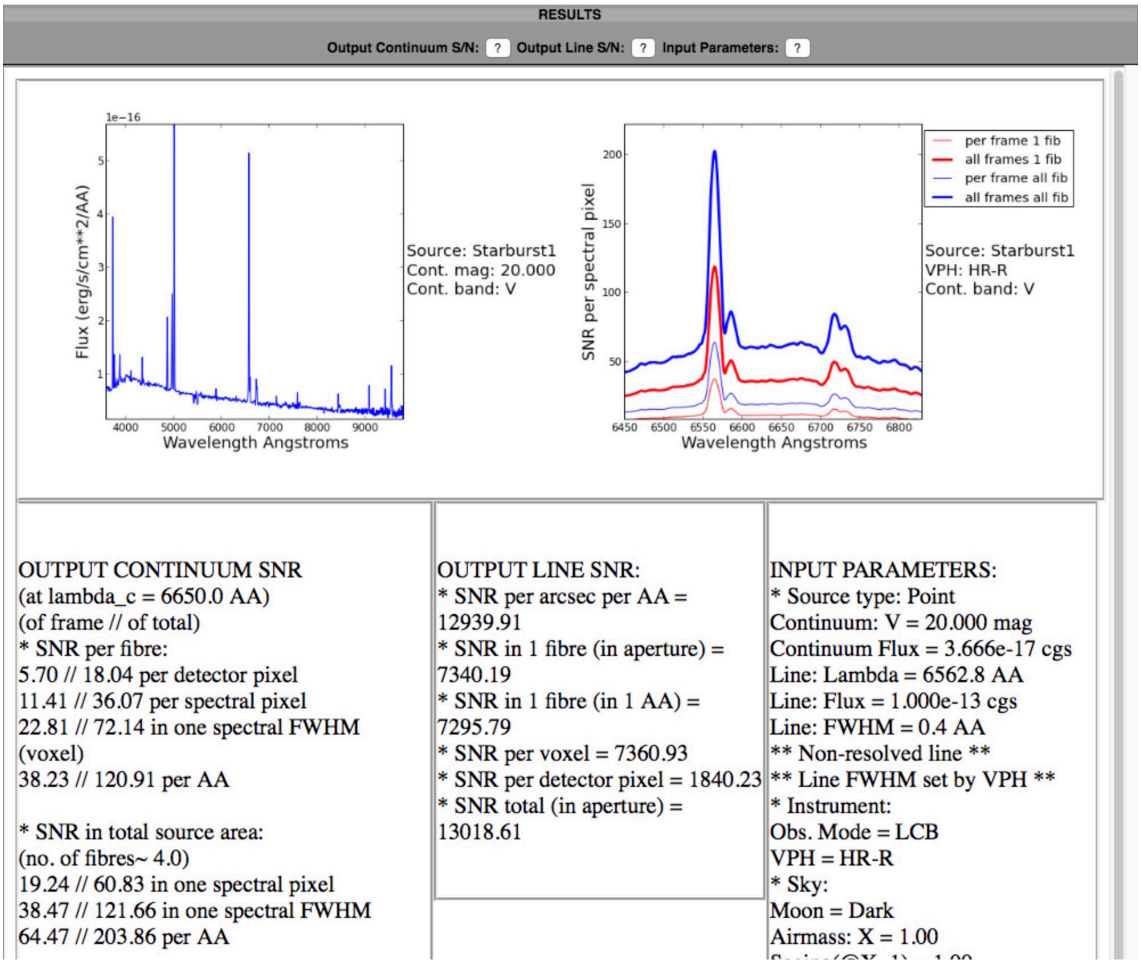


**Figure 12:** *Example outputs when input parameters are correct. A warning is given when the input parameters are incorrect, and no values are computed in that case.*

### 7.3.2. Line output SNRs

The current version of the ETC provides SNRs in an input line for an input parameters set.

In case we are dealing with a point source, the provided SNRs are for[6]:

- per arcsec and per Å in the detector[7].
- in one fiber (spaxel), in the selected spectral aperture[8];

---

6 Assuming that all the line flux is completely enclosed into the line FWHM.

7 Assuming a spectral aperture of 1 Å.

8 Assuming the selected spectral apertures for line and continuum subtraction provided as inputs. If you are interested in the SNR in 1 line FWHM, set the spectral apertures of line and continuum to 1 (i.e., to

- in one fiber (spaxel), per Å(4);
- per voxel(9,10);
- per detector pixel(11).
- the total source area, in the selected line spectral aperture(5).

In case of extended sources, the following outputs are additionally provided(3):

- for 1 arcsec$^2$, in the selected line spectral aperture(5).

Future improvements to the ETC will provide the exposure time required to get a given input SNR in the line for an input parameters set, or the limiting flux achieved for a given exposure time and SNR. An input option will allow the user to select the kind of required output. All these outputs will be provided considering the different spatial and spectral resolution elements on the detector listed above.

### 7.3.3. Graphical outputs

Graphical outputs can now be generated with the ETC online (see Figure 13) . These plots are generated using standard Python 2D plotting library *matplotlib*. We plot the total continuum flux of the source (left) over the whole wavelength range of the instrument. The flux is calculated from the input spectrum, the continuum band, the input continuum magnitude (or flux). We also plot the resulting SNR per spectral pixel (4 spatial pixels combined into one) i.e. per spaxel, computed at each wavelength over the VPH wavelength range. When “Num. frames” is larger than 1, the thin red line is the SNR per frame in 1 fiber, and the thick red line is the total SNR for the total exposure time in 1 fiber. Two more lines are shown, representing the SNR per frame for total area (thin blue), or for total exposure time (thick) for total area.

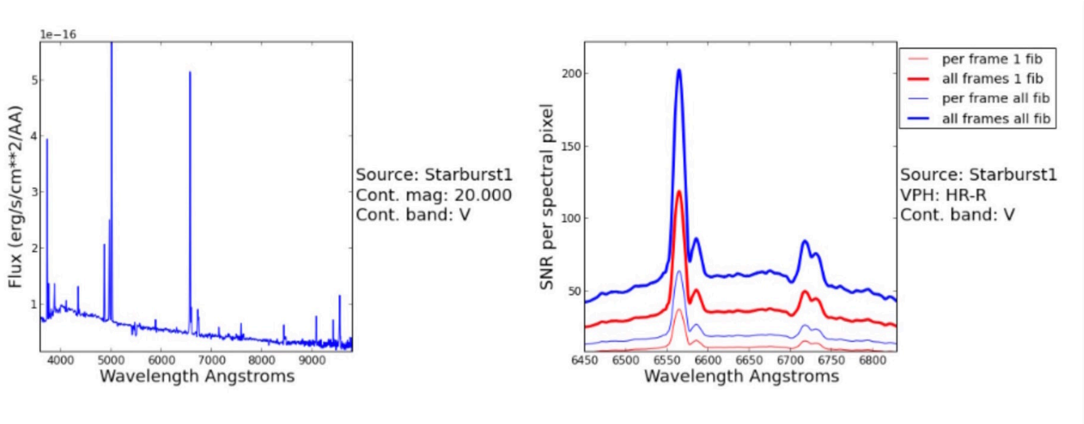


**Figure 13:** *Graphical outputs example. Left: source spectrum flux (in erg/s/cm$^2$/Å) versus wavelength (in*

---

one line FWHM).

[9] Assuming 4 spectral pixels as spectral aperture (i.e., the FWHM of the selected VPH).

[10] A voxel is the minimum spatial and spectral resolution element sampled. In our case, one voxel is the projection of the whole fiber (minimum spatial resolution element) and of the VPH FWHM (minimum spectral resolution element) into 4×4 spectral pixels in the detector (see §3.20).

[11] Assuming 1 spectral pixel as spectral aperture, the one with the best transmission in one voxel.

*Å). Right: resulting SNR per spectral pixel for: one frame and one fiber* ***(thin red)****, all frames and one fiber* ***(thick red)****, one frame and total area* ***(thin blue)****, and, all frames and total area* ***(thick blue)****.*

## 7.4. Physical model of the MEGARA ETC

### 7.4.1. Continuum SNRs formulae

The obtained formulas are based on those derived for the ETCs of ESO instruments [R.23, R.26]. The total number of photons received from certain target between wavelengths ($\lambda_1$, $\lambda_2$) is given by:

$$S = \int_{\lambda_1}^{\lambda_2} \frac{\mathcal{F}_{\rm arc}(\lambda) \cdot T(\lambda) \cdot S_{\rm t} \cdot \Omega_{\rm obj} \cdot t_{\rm exp}}{E_\phi(\lambda)}\, d\lambda \tag{11},$$

where $F_{arc}$ $(\lambda)$ is the flux per arcsec$^2$ of the target at each wavelength lambda, $T(\lambda)$ is the total transmission of the complete system at lambda, $S_t$ is the telescope collecting area, $\Omega_{obj}$ is the target projected area contributing to the signal, $E_\phi$ $(\lambda)$ is the energy of a photon with wavelength $\lambda$, and $t_{exp}$ is the exposure time. If the input target flux is inserted in c.g.s units per arcsec$^2$ (i.e., in erg/s/cm$^2$/Å, see §6.3), then the telescope area must be in cm$^2$, the target projected area in arcsec$^2$, the photon energy in erg, the exposure time in seconds, and the wavelengths in Å. The wavelengths $\lambda_1$ and $\lambda_2$ correspond to the initial and final wavelengths of the considered wavelength range in the detector plane. The two extreme wavelength values considered can be written as:

$$\lambda_1 = \lambda_0 - \frac{\Delta\lambda}{2} \qquad\qquad \lambda_2 = \lambda_0 + \frac{\Delta\lambda}{2} \tag{12}$$

being $\Delta\lambda = \lambda_2 - \lambda_1$ the considered wavelength range width, and $\lambda_0$ the central wavelength of this range. In the case of continuum, we consider that the wavelength range is always centered on the effective wavelength of the user-selected VPH (see *Table 1*).

In the case of a point source, the projected area of a source on the sky is the seeing disk. Assuming that all the flux of a point source is uniformly distributed into a circle of diameter equal to the seeing FWHM, the projected area of the point source is:

$$\Omega_{\rm obj} = A_{\rm seeing} \tag{13}$$

being $A_{seeing}$ the area of the seeing given by the following equation:

$$A_{\rm seeing} = \pi \left(\frac{\rm FWHM}{2}\right)^2 \tag{14}$$

Several possibilities have been considered for different $\Omega_{obj}$ depending on the output SNR that we have considered (see §7.4.2). The values assigned in each case to $\Omega_{obj}$ are listed in *Table 6* and *Table 7* in §7.4.2.

In the case of point sources, the user is requested to provide the total continuum flux in a certain band *i* as input $F_i$. Using the user-selected spectrum template and the selected VPH, MEGARA ETC derives the energy flux spectrum of the source *F(λ)* (in erg/s/cm$^2$/Å, see §6.3). Then, the energy flux per arcsec$^2$ of the source can be derived just dividing by the source projected size (i.e., the projected area of the seeing disk if it is a point source):

$$\mathcal{F}_{\rm arc}(\lambda) = \mathcal{F}(\lambda)/A_{\rm seeing} \quad .(15)$$

If the target is extended, the user-provided total continuum flux in a given input *i* band, $F_i$, should be provided per arcsec$^2$ (or, equivalently, the total continuum magnitude provided by the user is already per arcsec$^2$). Therefore, no normalization is required to get $F_{arc}(\lambda)$, once the selected template spectrum is adequately scaled to the input flux in the input *i* band (see §6.3).

The total transmission of the system accounts for the transmissions of the atmosphere $T_{atm}(\lambda)$, the telescope $T_{tel}(\lambda)$, and the instrument $T_{ins}(\lambda)$, as well as for the quantum efficiency of the detector $q_e(\lambda)$, as follows:

$$T(\lambda) = T_{\rm atm}(\lambda) \cdot T_{\rm tel}(\lambda) \cdot T_{\rm ins}(\lambda) \cdot q_{\rm e}(\lambda) \quad ,(16)$$

The transmission of the instrument considers the transmission of the optics at the current optical design ($T_{optics}(\lambda)$, see §6.2.2), the VPHs transmission ($T_{VPH}(\lambda)$, consult §6.2.3), and the fibers ($T_{fiber}(\lambda)$) in the following way:

$$T_{\rm ins}(\lambda) = T_{\rm optics}(\lambda) \cdot T_{\rm VPH}(\lambda) \cdot T_{\rm fibre}(\lambda) \quad ,(17)$$

The collecting area of the telescope is easily computed assuming the effective radius of the GTC telescope ($R_{t,eff}$ = 485.8 cm), through:

$$S_{\rm t} = \pi \cdot R_{\rm t,eff}^2 \quad ,(18)$$

The energy of a photon of wavelength λ is provided by the following equation:

$$E_\phi = \frac{hc}{\lambda} \quad ,(19)$$

being *h* the Planck constant ($h$=6.62606885 $\times 10^{27}$ ergs/s), and *c* the light speed ($c$=2.99792458 $\times 10^{10}$ cm/s). If the previous units are used, λ must be provided in cm.

Equivalently, the number of photons received from the sky emission (together with those coming from the source) will be:

$$S_{\text{sky}} = \int_{\lambda_1}^{\lambda_2} \frac{\mathcal{F}_{\text{arc,sky}}(\lambda) \cdot T(\lambda) \cdot S_{\text{t}} \cdot \Omega_{\text{obj,sky}} \cdot t_{\text{exp}}}{E_{\phi}(\lambda)} \, d\lambda \quad ,(20)$$

where $F_{arc,sky}$ *(λ)* is the sky flux per arcsec$^2$ at each wavelength lambda, and $\Omega_{obj,sky}$ is the sky projected area contributing to the target signal *S* in arcsec$^2$. Again, depending on the output SNR that we have considered, $\Omega_{obj,sky}$ adopts different values (consult *Table 6* and *Table 7* in §7.4.2 for the value used in each case for this parameter).

The error in the measurement of the signal *S* in Eq. 11 will be mainly due to the typical Poissonian error entailed by the source signal and the associated sky signal, to the readout noise, to the dark current, and to the error associated to the measurement of the sky signal and dark current. So, we can consider that the noise *N* of the signal *S* can be expressed as the quadratic sum of the various (independent) noise contributions [R.23, R.27]:

$$N = \sqrt{S + S_{\text{sky}} + S_{\text{dark}} + S_{\text{RON}} + N_{\text{SM}}^2 + N_{\text{DM}}^2} \quad .(21)$$

In the previous expression, we have already considered that the noise to the square associated to any photon signal (coming from the source, the sky, the dark current, or from the readout noise) is the signal itself *S*, i.e.: $\sigma_S^2=S$, $\sigma_{sky}^2=S_{sky}$, $\sigma_{dark}^2=S_{dark}$, and $\sigma_{RON}^2=S_{RON}$.

The source and the sky signals are given by Eqs. 11 and 20. The dark signal can be computed through the following expression:

$$S_{\text{dark}} = t_{\text{exp}} \cdot \text{DARK} \cdot n_{\text{pix,obj}} \quad ,(22)$$

where *DARK* is the value of the detector dark current in electrons/pix/s and $n_{pix,obj}$ is the number of detector pixels of the source considered in the detector plane. This last number is given by:

$$n_{\text{pix,obj}} = n_{\text{pix,y}} \cdot n_{\text{pix,x}} \quad ,(23)$$

being $n_{pix,y}$ and $n_{pix,x}$ the number of pixels considered in the spatial (*y*) and spectral (*x*) directions of the detector (whose values depend on the considered SNR case for being provided as output, as listed in *Table 6* and *Table 7* of §7.4.2).

The readout noise signal is:

$$S_{\text{RON}} = n_{\text{pix,obj}} \cdot \text{RON}^2 \quad ,(24)$$

being *RON* the rms of the detector readout noise in electrons.

The terms $N^2_{SM}$ and $N^2_{DM}$ in eq. 21, provide the error associated to the measurement of the sky signal and dark current (both of which scale inversely with the number of pixels used to determine them) and to the subsequent subtraction of these measured values to the obtained data, after applying the proper scaling to the considered target or sky projected area.

The average value of the sky measurement is scaled to the input data multiplying by the factor ($\Omega_{obj,sky}/\Omega_{sky}$), and thus the propagated error associated to the subtraction of this scaled value will be:

$$N_{\mathrm{SM}}^2 = \left(\frac{\Omega_{\mathrm{obj,sky}}}{\Omega_{\mathrm{sky}}}\right)^2 \cdot \left[S_{\mathrm{SM}} + n_{\mathrm{sky}} \cdot (\mathrm{RON})^2 + n_{\mathrm{sky}} \cdot \mathrm{DARK} \cdot t_{\mathrm{exp}}\right] \quad ,(25)$$

Equivalently to Eq. 21, the error associated to the sky measurement can be written as the quadratic sum of those (independent) error sources present in the measurement process: the Poissonian error associated to the sky photon flux, that due to the dark current, and that derived from the readout noise (that corresponds to the addends inside the square brackets in the previous equation, respectively). The measured sky signal will be given by an expression similar to eq. 20, but considering the total sky projected area used for determining it, $\Omega_{sky}$:

$$S_{\mathrm{SM}} = \int_{\lambda_1}^{\lambda_2} \frac{\mathcal{F}_{\mathrm{arc,sky}}(\lambda) \cdot T(\lambda) \cdot S_{\mathrm{t}} \cdot \Omega_{\mathrm{sky}} \cdot t_{\mathrm{exp}}}{E_{\phi}(\lambda)} \, d\lambda \quad . (26)$$

Here, $F_{arc,sky}(\lambda)$ represents the energy flux per arcsec$^2$ of the sky. The total sky area used $\Omega_{sky}$ depends on the number of sky fiber mini-bundles $N_{sky,bundles}$ considered by the user, as:

$$\Omega_{\mathrm{sky}} = N_{\mathrm{sky,fibers}} \cdot A_{\mathrm{fibre}} \quad ,(27)$$

where $N_{sky,fibers}$ is the total number of sky fibers used ($N_{sky,fibers}$ = 7 fibers × $N_{sky,bundles}$), and $A_{fiber}$ is the sky-projected area of a MEGARA fiber (see §3.4).

The term $n_{sky}$ in Eq. 25 represents the number of detector pixels used to derive the sky signal measurement, and it is equal to the product of the pixels considered in the spectral direction ($n_{sky,x}$) by the number of pixels considered in the spatial direction ($n_{sky,y}$):

$$n_{\mathrm{sky}} = n_{\mathrm{sky,y}} \cdot n_{\mathrm{sky,x}} \quad , (28)$$

where $n_{sky,x}=n_{pix,x}$ because in both cases we are considering the same spectral range, and $n_{sky,y}=4\times N_{sky,fibers}$ because we are considering the projected spectra of all the used sky fibers and each fiber projects onto 4 pixels in the spatial direction (y) of the detector [R.5, R.12]. The adopted value of $n_{pix,x}$ depends on the case of output SNR considered. The values assigned to this paremeter for each output SNR case are listed in *Table 6* and *Table 7* of §7.4.2.

The average value of the measured dark is scaled to the input data by the factor ($n_{pix,obj}$ /$n_{dark}$), being $n_{dark}$ the number of pixels used to determine the dark current (this value is fixed in the MEGARA ETC to $n_{dark}$ = 256×256 = 65536, TBC). Therefore, the propagated error associated to the subtraction of this scaled value will be:

$$N_{\mathrm{DM}}^2 = \left(\frac{n_{\mathrm{pix,obj}}}{n_{\mathrm{pix,dark}}}\right)^2 \cdot \left[t_{\mathrm{exp}} \cdot \mathrm{DARK} \cdot n_{\mathrm{pix,dark}} \cdot + n_{\mathrm{pix,dark}} \cdot (\mathrm{RON})^2\right] \quad . (29)$$

In the previous expression, the first addend into the square brackets represents the dark signal measured to determine the average dark signal, while the second addend is the readout noise entailed by this measurement.

Once we have estimated Eqs. 11 and 21, the SNR of the continuum of the input source can be derived just dividing the signal by the noise:

$$\mathrm{SNR} = \frac{S}{N} \quad . \tag{30}$$

### 7.4.2. Spectral and spatial parameters for continuum SNR estimates

In the present version of MEGARA ETC, the flux in a fiber is assumed to be projected uniformly along 4 pixels in the spatial direction of the detector. The spectral projection of the fiber on the detector is assumed to be uniform too. Nevertheless, the total signal in the voxel is quite similar considering this uniform flux distribution and a more realistic one, so we do not expect a significant change in the estimates assuming corrections due to the different distribution of one fiber flux onto each one of these 4 pixels (because of the geometric section of the project of the fiber on the detector across the spatial direction) [R.47], although they could be considered in future versions (TBD).

However, the current tool estimates the SNR in the central pixel of the voxel in the spatial direction, considering the percentage of flux corresponding to it: 32.82% in the fibers of 100 microns, for the 4 spectral pixels in a voxel [R.47]. This means that the output SNR estimates per pixel on the detector provide the maximum SNR achieved in one of the pixels in a voxel.

In Table *6*, we show the values assigned to the different parameters in Eqs. 11-30 for deriving the output continuum SNRs provided by MEGARA ETC for ***point*** sources. Different spatial and spectral elements onto the detector have been considered, as well as different projected areas on the punctual source contributing to the signal. The central wavelength $\lambda_0$ in all the cases will correspond to the effective wavelength of the selected VPH. In Table *6*, *D* represents the dispersion of the selected VPH, *PS* is the MEGARA detector plate scale (*PS* = 0.17 arcsec/pix), $\Delta B$ is the width of the spectral range of the VPH, and $A_{fiber}$ and $R_{eff,fiber}$ are the projected area and the "effective" radius of the hexagonal fiber in arcsec$^2$, respectively (consult §3.4). The effective radius of the hexagonal fiber corresponds to the radius of a circular fiber with the same area of the cross section as our hexagonal fiber, i.e.:

$$R_{eff,fiber} = \sqrt{\frac{3\sqrt{3}}{2\pi}} L_{spaxel} \quad . \tag{31}$$

For the parameters related to the user-selected VPH see *Table 1*.

In Table *7*, we show the values assigned to the different parameters in Eqs. 11-30 for deriving the output continuum SNRs provided by MEGARA ETC for ***extended*** sources. As in the case of point sources, different spatial and spectral elements onto the detector have been considered, as well as different projected areas on the extended source contributing to the signal. Again, the central wavelength $\lambda_0$ is assumed to correspond to the effective wavelength of the selected VPH. In Table *7*, the parameters $D$, $\Delta B$, $A_{fiber}$ and $R_{eff,fiber}$ represent the same as in Table *6*.

If the source is extended, the problem can be translated to a point source problem in the following cases:

- If input target is extended and its diameter [12] is lower than the input seeing FWHM (i.e., if $R_{source} < FWHM/2$).
- If the target is extended and its diameter [9] and the seeing FWHM are contained within a fiber (i.e., if $R_{source} < R_{fiber}$ and $FWHM/2 < R_{fiber}$).

If any of these two cases occurs, a warning is sent to the user.

[12] The extended sources are assumed to exhibit a circular projected area. The radius of an extended source is derived from the input source area as follows: $R_{source} = \sqrt{(A_{source}/\pi)}$

.

***Table 6:*** *Values assigned to different photometric parameters in order to derive the output continuum SNRs provided by the MEGARA ETC for point sources.*

| **VALUES OF SPECTRAL AND SPATIAL PARAMETERS TO OBTAIN DIFFERENT CONTINUUM SNRs FOR POINT SOURCES** (*) | | **No. of pixels in the detector spectral direction (x)** | | | | |
|---|---|---|---|---|---|---|
| | | FWHM of VPH:<br>$\Delta\lambda = 4D$<br>$n_{pix,x} = 4$ pixels | $N_{pix}$ in 1 Å:<br>$\Delta\lambda = 1$ Å<br>$n_{pix,x} = 1/D$ | $N_{pix}$ in whole spectrum:<br>$\Delta\lambda = \Delta B$<br>$n_{pix,x} = \Delta B/D$ | | |
| **Source and sky projected area contributing to emission in the projected element considered** | Total source area:<br>$\Omega_{obj} = A_{seeing}$<br>Sky emission:<br>- If $FWHM < 2R_{fiber} \Rightarrow$ $\Omega_{obj,sky} = A_{fiber}$<br>- If $FWHM \geq 2R_{fiber} \Rightarrow$ $\Omega_{obj,sky} = A(N_{fibers})$ (**) | | | Total SNR of source, λ-collapsed spectrum | $N_{pix}$ in total projected source in y(**):<br>- If $FWHM < 2R_{fiber} \Rightarrow n_{pix,y} = 2R_{eff,fiber}/PS$<br>- If $FWHM \geq 2R_{fiber} \Rightarrow n_{pix,y} = N_{fibers} \times [2 \times R_{eff,fiber}/PS]$ | **No. of pixels considered in the detector spatial direction (y)** |

Multi Espectrógrafo en GTC de Alta Resolución para Astronomía

| | | | | | | |
|---|---|---|---|---|---|---|
| | Source emission in 1 projected fiber:<br>- If $FWHM < 2R_{fiber} \Rightarrow \Omega_{obj}=A_{seeing}$<br>- If $FWHM \geq 2R_{fiber} \Rightarrow \Omega_{obj}=A_{fiber}$<br>Sky emission: $\Omega_{obj,sky}= A_{fiber}$ | SNR in 1 fiber, per FWHM of VPH<br>**(1 voxel)** | SNR in 1 fiber, per Å | SNR in 1 fiber, λ-collapsed spectrum<br>**(1 spaxel)** | $N_{pix}$ in one projectedfiber in y (4 y-pixels):<br>$n_{pix,y} = 2\ R_{eff,fiber}/PS = 4$ pixels | |
| | | 1 x-pixel: $\Delta\lambda = 1D$ , $n_{pix,x} = 1$ pixel | | | | |
| | Source emission in 1 y-pixel of a projected fiber(***):<br>- *If* $FWHM < 2R_{fiber} \Rightarrow \Omega_{obj}=A_{seeing}$<br>– *If* $FWHM \geq 2R_{fiber} \Rightarrow S$*(in 1 y-pixel) = S(in 1 spaxel /[no. Pixels in one voxel] if uniform distribution*<br>– *If not, 32.82% in the fibers of 100 micron divided into the number of pixels of the FWHM in the spectral direction*<br>Sky emission: $S_{sky}$*(in 1 y-pixel) =* $S_{sky}$ *(in 1 spaxel)/[no. Pixels in one voxel/*spaxel*]* | SNR in 1 detector pixel<br>(the central one of the voxel, considering the maximum flux distribution within the spatial profile of a projected fiber) | | | 1 y-pixel:<br>$n_{pix,y} = 1$ pixel | |

**Table notes:**

(*) The flux in a fiber is assumed to be projected uniformly along 4 pixels in the spatial direction of the detector. The spatial projection of the fiber on the detector is assumed to be flat, except for the estimates in one pixel, in which the pixel with the maximum signal in a voxel is provided.

(**) The area of all the required fibers to ensure a complete coverage of the source will be noted $A(N_{fibers})$ hereafter. In this case, this area is: $A(N_{fibers})=A_{fiber}\ N_{fibers}$, where $N_{fibers}$ computes the integer number of fibers required to cover the seeing disk. We will note as "FLOOR" to the function that returns the nearest and highest integer of a given decimal value, then: $N_{fibers}$ = FLOOR$(A_{seeing}/A_{fiber})$.

| |
|---|
| (***) The signal in one detector pixel is computed from the signal in one voxel, considering that the light distribution in the spatial profile of a voxel has a maximum of flux in its central pixel of 32.82% in the fibers of 100 micron, for all the pixels in the voxel in the spectral direction. |

***Table** 7: Values assigned to different photometric parameters in order to derive the output continuum SNRs provided by the MEGARA ETC for extended sources.*

| **VALUES OF SPECTRAL AND SPATIAL PARAMETERS TO OBTAIN DIFFERENT CONTINUUM SNRs FOR EXTENDED SOURCES[*]** | | **No. of pixels considered in the detector spectral direction (x)** | | | | |
|---|---|---|---|---|---|---|
| | | FWHM of VPH:<br>$\Delta\lambda = 4D$<br>$n_{pix,x} = 4$ pixels | $N_{pix}$ in 1 Å:<br>$\Delta\lambda = 1$ Å<br>$n_{pix,x} = 1/D$ | $N_{pix}$ in whole spectrum:<br>$\Delta\lambda = \Delta B$<br>$n_{pix,x} = \Delta B/D$ | | |
| **Source and sky projected area contributing to emission in the considered projected element** | Total source area: $\Omega_{obj}= A_{obj}$ (user input)<br>Sky emission[**]: $\Omega_{obj,sky}= A(N_{fibers})$ | | | Total SNR of source, λ-collapsed spectrum | $N_{pix}$ in total projected source in y[**]:<br>$n_{pix,y} = N_{fibers} \times [2\times R_{eff,fiber} /PS]$ | **No. of pixels considered in the detector spatial direction (y)** |
| | Source emission in 1 projected fiber: $\Omega_{obj}=A_{fiber}$<br>Sky emission: $\Omega_{obj,sky}= A_{fiber}$ | SNR in 1 fiber, per FWHM of VPH<br>**(1 voxel)** | SNR in 1fiber, per Å | SNR in 1 fiber, λ-collapsed spectrum<br>**(1 spaxel)** | $N_{pix}$ in 1 spaxel in y (4 y-pixels):<br>$n_{pix,y} = 2R_{eff,fiber}/PS = 4$ pixels | |
| | Emission in 1 arcsec$^2$:<br>- If $A_{obj} < 1\ arcsec^2 \Rightarrow \Omega_{obj}=A_{obj}$<br>- If $A_{obj} \geq 1\ arcsec^2 \Rightarrow \Omega_{obj}=1\ arcsec^2$<br>Sky emission: $\Omega_{obj,sky} = 1\ arcsec^2$ | | SNR per arcsec per Å on the detector | SNR in 1 arcsec$^2$, λ-collapsed spectrum | $N_{pix}$ in 1 y-projected arcsec$^2$:<br>$n_{pix,y} = FLOOR[1arcsec^2/A_{fiber}] \times [2\times R_{eff,fiber} /PS]$ | |
| | | 1 x-pixel: $\Delta\lambda = D$ , $n_{pix,x} = 1$ pixel | | | | |

| | | | | |
|---|---|---|---|---|
| | Source emission in 1 y-pixel of a projected fiber(***):<br>- *If FWHM* $< 2R_{fiber} \Rightarrow \Omega_{obj}=A_{seeing}$<br>- *If FWHM* $\geq 2R_{fiber} \Rightarrow$ *(in 1 y-pixel) = S(in 1 spaxel /[no. Pixels in one voxel] if uniform distribution.*<br>*If not, 32.82% in the fibers of 100 micron divided into the number of pixels of the FWHM in the spectral direction.*<br>Sky emission: $S_{sky}$*(in 1 y-pixel) =* $S_{sky}$ *(in 1 spaxel)/[16 pix/sp*x] | SNR in 1 detector pixel<br>(the central one of the voxel, considering the maximum flux distribution within the spatial profile of a projected fiber) | 1 y-pixel:<br>$n_{pix,y} = 1$ | |

**Table notes:**

(*) The projected area of the extended source is assumed to be circular.

(**) The area of all the required fibers to ensure a complete coverage of the source will be noted $A(N_{fibers})$ hereafter. In this case, this area is: $A(N_{fibers})=A_{fiber}\ N_{fibers}$, where $N_{fibers}$ computes the integer number of fibers required to cover the source. We will note as "FLOOR" to the function that returns the nearest and highest integer of a given decimal value, then: $N_{fibers}$ = FLOOR$(A_{obj}/A_{fiber})$.

### 7.4.3. Line SNRs formulae

The formulas for deriving SNRs of an emission line are equivalent to those derived for the continuum emission (see §7.4.1). Now, the signal (i.e., the number of photons) detected by GTC+MEGARA in the selected configuration in the whole line (independently of the line FWHM, $FWHM_{line}$, which is a user-selected input, see §4) is:

$$S_{\rm line} = \frac{\mathcal{F}_{\rm arc}(\lambda_0) \cdot T(\lambda_0) \cdot S_{\rm t} \cdot \Omega_{\rm obj} \cdot t_{\rm exp}}{E_\phi(\lambda_0)} \quad , (32)$$

being $T(\lambda_0)$ the transmission of the whole system at the line wavelength $\lambda_0$ (see Eqs. 16-(17), $S_t$ the telescope collecting area (see Eq. ,(18), $\Omega_{obj}$ is the target projected area contributing to the signal, $E_\phi(\lambda_0)$ is the energy of a photon with wavelength $\lambda_0$ (see Eq. 19), and $t_{exp}$ is the exposure time.

In this case, the line wavelength $\lambda_0$ is given by the user as input. $F_{arc}(\lambda_0)$ is the energy flux emitted by the target at the line wavelength per arcsec$^2$. The user is requested to provide as input the integrated energy flux of the line if the object is a point source, $F(\lambda_0)$, or per arcsec$^2$ if the source is extended, $F_{arc}(\lambda_0)$. In the former case, its projected area is determined by the seeing disk. Again, $F_{arc}(\lambda_0)$ is estimated from $F(\lambda_0)$ and the input FWHM of the seeing through Eqs. 13-15.

Several possibilities have been considered for different $\Omega_{obj}$ depending on the output SNR that we have considered (see §7.4.4). The values assigned in each case to $\Omega_{obj}$ are listed in *Table 8* and *Table 9* in §7.4.4.

The noise contributing to the line signal in the considered spectral aperture (provided as input by the user in $FWHM_{line}$ units, see §5) will be given by the square root of the quadratic summation of all the independent noise sources contributing to the derivation of the line signal in the spectrum:

$$N_{\rm line} = \sqrt{S_{\rm line} + S_{\rm cont} + S_{\rm dark} + S_{\rm RON} + N_{\rm CS}^2 + N_{\rm DS}^2} \quad .(33)$$

The first four addends inside the square root correspond to the photon noises associated to the line signal, continuum signal, dark current, and readout noise in the considered spectral aperture, respectively. $N_{CS}$ and $N_{DS}$ symbolize the noises due to continuum-subtraction using the continuum spectral aperture (provided by the user as input, in $FWHM_{line}$ units, see §6) and dark-subtraction in the spectrum, respectively.

Let us call $\Delta\lambda_{line}$ to the line spectral aperture considered on the detector. This aperture can adopt different values, depending on the output SNR that we are interested in (it can be one spectral pixel, one Å, one $FWHM_{line}$, or the user-selected line spectral aperture, see §7.4.4 for the values used in each output case). If the user-selected spectral aperture is used, then this line spectral aperture is given by:

$$\Delta\lambda_{\rm line} = n_{\rm line} \cdot {\rm FWHM}_{\rm line}$$ ,(34)

where $n_{line}$ is the number inserted by the user of line FWHMs to be considered around the central line wavelength as aperture for deriving the line signal (see §5). The user-selected spectral aperture for continuum subtraction $\Delta\lambda_{CS}$ is computed in a similar way, through:

$$\Delta\lambda_{\rm CS} = n_{\rm CS} \cdot {\rm FWHM}_{\rm line}$$ , (35)

being $n_{CS}$ the number of line FWHMs considered by the user to subtract continuum emission (see §6).

The continuum signal inside this aperture will contribute to the line noise, according to Eq. 33. This can be estimated similarly to Eq. 11, but now considering the spectral aperture around the line wavelength $\lambda_0$:

$$S_{\rm cont} = \int_{\lambda_0-\Delta\lambda_{\rm line}/2}^{\lambda_0+\Delta\lambda_{\rm line}/2} \frac{\mathcal{F}_{\rm arc}(\lambda) \cdot T(\lambda) \cdot S_{\rm t} \cdot \Omega_{\rm obj} \cdot t_{\rm exp}}{E_{\phi}(\lambda)}\, d\lambda$$ .(36)

The dark signal $S_{DARK}$ in Eq. 33 can be estimated as follows:

$$S_{\rm dark} = t_{\rm exp} \cdot {\rm DARK} \cdot n_{\rm pix,\Delta\lambda_{line}}$$ , (37)

where we must account for the number of pixels considered on the detector $n_{pix,\Delta\lambda line}$. This depends on the number of pixels considered in the spectral and spatial directions of the detector:

$$n_{\rm pix,\Delta\lambda_{line}} = n_{\rm pix,x}(\Delta\lambda_{\rm line}) \cdot n_{\rm pix,y}$$ . (38)

The number of pixels in the spectral direction $n_{pix,x}(\Delta\lambda_{line})$ depends directly on the spectral aperture considered through the dispersion of the selected VPH ($D$), according to:

$$n_{\rm pix,x}(\Delta\lambda_{\rm line}) = \Delta\lambda_{\rm line}/D$$ . (39)

Different values of $n_{pix,x}(\Delta\lambda_{line})$ and $n_{pix,y}$ depending on the considered spectral aperture and spatial elements to provide the output line SNR are listed in *Table 8* and *Table 9* in §7.4.4.

The readout signal $S_{RON}$ in Eq. 33 will also depend on the number of pixels considered on the detector, as:

$$S_{\mathrm{RON}} = n_{\mathrm{pix},\Delta\lambda_{\mathrm{line}}} \cdot \mathrm{RON}^2 \quad . (40)$$

The noise due to continuum-subtraction obtained in the aperture $\Delta\lambda_{CS}$ must be scaled to aperture where the signal is estimated $\Delta\lambda_{line}$, by multiplying by the factor ($\Delta\lambda_{line}/\Delta\lambda_{CS}$). This implies that the propagated error associated to the subtraction of this scaled value will be:

$$N_{\mathrm{CS}}^2 = \left(\frac{n_{\mathrm{line}}}{n_{\mathrm{CS}}}\right)^2 \cdot N_{\mathrm{cont}}^2(\Delta\lambda_{\mathrm{CS}}) \quad . \quad (41)$$

In the previous expression, $N^2_{cont}$ *($\Delta\lambda_{CS}$)* represents the squared noise corresponding to the continuum in a spectral aperture $\Delta\lambda_{CS}$ on the detector, which is estimated through Eq. 21, as indicated in §7.4.1. For this computation, the continuum-spectrum aperture $\Delta\lambda_{CS}$ must be assumed in order to estimate all the contributions to $N^2_{cont}$ *($\Delta\lambda_{CS}$)* (see §7.4.1). In particular, the first addend inside the square root in Eq. 21 (the continuum signal, *S*) would be in this case:

$$S_{\mathrm{cont}} = \int_{\lambda_0-\Delta\lambda_{\mathrm{CS}}/2}^{\lambda_0+\Delta\lambda_{\mathrm{CS}}/2} \frac{\mathcal{F}_{\mathrm{arc}}(\lambda) \cdot T(\lambda) \cdot S_{\mathrm{t}} \cdot \Omega_{\mathrm{obj}} \cdot t_{\mathrm{exp}}}{E_\phi(\lambda)}\, d\lambda \quad (42)$$

The number of pixels, $n_{pix,\Delta\lambda CS}$, to be considered when estimating $N^2_{cont}$ *($\Delta\lambda_{CS}$)* will be:

$$n_{\mathrm{pix},\Delta\lambda_{\mathrm{CS}}} = n_{\mathrm{pix,x}}(\Delta\lambda_{\mathrm{CS}}) \cdot n_{\mathrm{pix,y}} \quad , (43)$$

where $n_{pix,x}$ is set by the continuum-subtraction aperture selected by the user through:

$$n_{\mathrm{pix,x}}(\Delta\lambda_{\mathrm{CS}}) = \Delta\lambda_{\mathrm{CS}}/D \quad . (44)$$

The last term inside the square root of Eq. 33 (the noise due to dark subtraction) will be:

$$N_{\mathrm{DS}}^2 = \left(\frac{n_{\mathrm{pix},\Delta\lambda_{\mathrm{line}}}}{n_{\mathrm{pix,dark}}}\right)^2 \cdot \left[t_{\mathrm{exp}} \cdot \mathrm{DARK} \cdot n_{\mathrm{pix,dark}} \cdot + n_{\mathrm{pix,dark}} \cdot (\mathrm{RON})^2\right] \quad , (45)$$

where the term ($n_{pix,\Delta\lambda line}/n_{pix,dark}$) comes from the scaling of the average dark signal computed to the number of pixels in the considered spectral aperture (this is analogous to Eq. 29).

Finally, the output line SNR is estimated through Eqs. 32 and 33, as follows:

$$\mathrm{SNR}_{\mathrm{line}} = \frac{S_{\mathrm{line}}}{N_{\mathrm{line}}} \quad . (46)$$

#### 7.4.4. Spectral and spatial parameters for line SNR estimates

As commented in §7.4.2, in the present version of MEGARA ETC, the flux in a fiber is assumed to be projected uniformly along 4 pixels in the spatial direction of the detector, and the spatial projection of the fiber on the detector is assumed to be flat. This provides a good approximation for total SNR estimates in a voxel or in one spaxel. Corrections due to the different distribution of one fiber flux onto each one of these 4 pixels (because of the geometric section of the fiber) will be implemented in future versions. Anyway, the SNR per detector pixel is provided for the central pixel of the voxel, which accumulates 32.82% of the flux in the fibers of 100 microns considering the Gaussian distribution of light in the spatial direction in one voxel, integrated for the 4 spectral pixels in a voxel [R.47]. This means that the output SNR estimates per pixel on the detector provide the maximum SNR achieved in one of the pixels in a voxel.

In *Table 8* and *Table 9*, we list the values assigned to the different parameters in Eqs. 32-46 for deriving the output line SNRs provided by MEGARA ETC for *point* and *extended* sources, respectively. Different spatial and spectral elements onto the detector have been considered, as well as different projected areas on the source contributing to the signal. The central wavelength $\lambda_0$ in all the cases corresponds to the line wavelength (input provided by the user). In the Tables 8 and 9, $D$ represents the dispersion of the selected VPH, $PS$ is the MEGARA detector plate scale ($PS$ = 0.17 arcsec/pix), $\sigma_{\mathrm{line}}$ is the line FWHM[13] (also provided by the user, see §11), and $A_{fiber}$ and $R_{eff,fiber}$ are the area and the "effective" radius of the hexagonal fiber, respectively (see eq. 31). For the parameters related to the user-selected VPH, see *Table 1*.

As noted above, if the source is extended, the problem can be translated to a point source problem in the following cases:

- If input target is extended and its diameter[(9)] is lower than the input seeing FWHM (i.e., if $R_{source}$ < FWHM/2).
- If the target is extended and its diameter and the seeing FWHM are contained in a fiber (i.e., if $R_{source} < R_{fiber}$ and FWHM/2< $R_{fiber}$).

If any of these two cases occurs, a warning indicating this is sent to the user.

If the output SNR is assuming 1 Å as spectral aperture, then the line signal per Å on the detector in the considered spatial element can be estimated through:

[13] We will note the line FWHM as $\sigma_{\mathrm{line}}$ or $\mathrm{FWHM}_{\mathrm{line}}$ indistinctly.

$$S_{\text{line},\mathring{\text{A}}} = \frac{S_{\text{line}}}{\text{FWHM}_{\text{line}}} \quad , (47)$$

where $S_{line}$ has been estimated through Eq. 32 and $\text{FWHM}_{\text{line}}$ is a user input (see §4).

If a spectral aperture of 1 spectral pixel were considered instead, the signal per spectral pixel in the considered spatial element would be:

$$S_{\text{line,spect-pix}} = S_{\text{line},\mathring{\text{A}}} \cdot D \quad . (48)$$

However, note that we provide the SNR in the central pixel of the voxel considering that it concentrates 32.82% of the flux in the fibers of 100 microns, according to the Gaussian distribution of light in the spatial direction in one voxel [R.47]. The previous value considers a uniform distribution of light in both the spatial and spectral direction of the voxel. Therefore, this value is thus scaled to account for this.

***Table 8**: Values assigned to different photometric parameters in order to derive the output line SNRs provided by the MEGARA ETC for point sources.*

| **VALUES OF SPECTRAL AND SPATIAL PARAMETERS TO OBTAIN DIFFERENT LINE SNRs FOR POINT SOURCES(*)** | | **No. of pixels considered in the detector spectral direction (x)** | | | | |
|---|---|---|---|---|---|---|
| | | Selected line aperture:<br>$\Delta\lambda = n_{line}\ \sigma_{line}$<br>$n_{pix,x} = n_{line}\ \sigma_{line} / D$ | FWHM of VPH:<br>$\Delta\lambda = 4D$<br>$n_{pix,x} = 4$ pixels | In 1 Å:<br>$\Delta\lambda = 1$ Å<br>$n_{pix,x} = 1/D$ | | |
| **Source and sky projected area contributing to the emission in the projected element** | Total source area: $\Omega_{obj} = A_{seeing}$<br>Sky emission:<br>- If FWHM < $2R_{fiber} \Rightarrow \Omega_{obj,sky} = A_{fiber}$<br>- If FWHM≥ $2R_{fiber} \Rightarrow \Omega_{obj,sky} = A(N_{fibers})$ (**) | Total SNR of source, in selected spectral aperture | | | $N_{pix}$ in total projected source in y(**):<br>- If FWHM < $2R_{fiber} \Rightarrow$<br>$n_{pix,y} = 2R_{eff,fiber}/PS$<br>- If FWHM ≥ $2R_{fiber} \Rightarrow$<br>$n_{pix,y} = N_{fibers} \times [2 \times R_{eff,fiber}/PS]$ | **No. of pixels considered in the detector spatial direction (y)** |
| | Source emission in 1 projected fiber:<br>- If $FWHM < 2R_{fiber} \Rightarrow \Omega_{obj} = A_{seeing}$<br>- If $FWHM \geq 2R_{fiber} \Rightarrow \Omega_{obj} = A_{fiber}$<br>Sky emission: $\Omega_{obj,sky} = A_{fiber}$ | SNR in 1 fiber, in selected spectral aperture<br>**(1 spaxel for spectral aperture)** | SNR in 1 fiber, per FWHM of VPH<br>**(1 voxel)** | SNR in 1 fiber, per Å | $N_{pix}$ in 1 spaxel in y (4 y-pixels):<br>$n_{pix,y} = 2R_{eff,fiber}/PS = 4$ pixels | |
| | 1 arcsec$^2$:<br>- If $A_{obj} < 1$ arcsec$^2 \Rightarrow \Omega_{obj} = A_{obj}$<br>- If $A_{obj} \geq 1$ arcsec$^2 \Rightarrow \Omega_{obj} = 1$ arcsec$^2$<br>Sky emission: $\Omega_{obj,sky} = 1$ arcsec$^2$ | | | SNR per arcsec per Å | $N_{pix}$ in 1 y-projected arcsec$^2$:<br>$n_{pix,y}$ =<br>FLOOR$[1 arcsec^2/A_{fiber}] \times [2 \times R_{eff,fiber}/PS]$ | |

| | | | | |
|---|---|---|---|---|
| | | 1 x-pixel: $\Delta\lambda = D$ , $n_{pix,x} = 1$ pixel | | |
| | Source emission in 1 y-pixel of a projected fiber(***):<br>- *If FWHM* < $2R_{fiber} \Rightarrow \Omega_{obj}=A_{seeing}$<br>- *If FWHM* ≥ $2R_{fiber} \Rightarrow$ S(in 1 y-pixel) = *S(in 1 spaxel /[no. Pixels in one voxel] if uniform distribution.*<br>*If not, 32.82% in the fibers of 100 micron divided into the number of pixels of the FWHM in the spectral direction.*<br>Sky emission:<br>$S_{sky}$*(in 1 y-pixel)* = $S_{sky}$ (in 1 spaxel) / *[16* pix/spx*]* | SNR in 1 detector pixel<br>(the central one of the voxel, assuming maximum light distribution in the spatial profile, but uniform light distribution in the spectral direction) | 1 y-pixel:<br>$n_{pix,y} = 1$ pixel | |

Notes:

(*) The flux in a fiber is assumed to be projected uniformly along 4 pixels in the spatial direction of the detector for voxel and spaxel estimates. The spatial projection of the fiber on the detector is thus assumed to be flat, except for estimates on the SNR in one pixel at the center of the voxel. Corrections due to the different distribution of one fiber flux onto each one of these 4 pixels (because of the geometric section of the fiber) could be implemented in future versions (TBD).

(**) The area of all the required fibers to ensure a complete coverage of the source will be noted $A(N_{fibers})$ hereafter. In this case, this area is: $A(N_{fibers})=A_{fiber}\ N_{fibers}$, where $N_{fibers}$ computes the integer number of fibers required to cover the seeing disk. We will note as "FLOOR" to the function that returns the nearest and highest integer of a given decimal value, then: $N_{fibers}$ = FLOOR$(A_{seeing}/A_{fiber})$.

(***) The signal in one detector pixel is computed from the signal in one voxel, considering that the light distribution in the spatial profile of a voxel has a maximum of flux in its central pixel of 32.82% in the fibers of 100 micron, for all the pixels in the voxel in the spectral direction.

***Table 9****: Values assigned to different photometric parameters in order to derive the output line SNRs provided by the MEGARA ETC for extended sources.*

| **VALUES OF SPECTRAL AND SPATIAL PARAMETERS TO OBTAIN DIFFERENT LINE SNRs FOR EXTENDED SOURCES(*)** | | **No. of pixels considered in the detector spectral direction (x)** | | | | |
|---|---|---|---|---|---|---|
| | | Selected line aperture:<br>$\Delta\lambda = n_{line}\ \sigma_{line}$<br>$n_{pix,x} = n_{line}\ \sigma_{line} / D$ | FWHM of VPH:<br>$\Delta\lambda = 4D$<br>$n_{pix,x} = 4$ pixels | In 1 Å:<br>$\Delta\lambda = 1$ Å<br>$n_{pix,x} = 1/D$ | | |
| **Source and sky projected area contributing to emission in the projected element considered** | Total source area: $\Omega_{obj} = A_{obj}$ (user input)<br>Sky emission(**): $\Omega_{obj,sky} = A(N_{fibers})$ | Total SNR of source, in selected spectral aperture | | | $N_{pix}$ in total projected source in y(**):<br>- If FWHM < $2R_{fiber} \Rightarrow$<br>$n_{pix,y} = 2R_{eff,fiber}/PS$<br>- If FWHM ≥ $2R_{fiber} \Rightarrow$<br>$n_{pix,y} = N_{fibers} \times [2 \times R_{eff,fiber}/PS]$ | **No. of pixels considered in the detector spatial direction (y)** |
| | Source emission in 1 projected fiber:<br>$\Omega_{obj} = A_{fiber}$<br>Sky emission: $\Omega_{obj,sky} = A_{fiber}$ | SNR in 1 fiber, in selected spectral aperture<br>**(1 spaxel for spectral aperture)** | SNR in 1 fiber, per FWHM of VPH<br>**(1 voxel)** | SNR in 1 fiber, per Å | $N_{pix}$ in 1 spaxel in y (4 y-pixels):<br>$n_{pix,y} = 2R_{eff,fiber}/PS = 4$ *pixels* | |
| | Emission in 1 arcsec$^2$:<br>- If $A_{obj} < 1$ arcsec$^2 \Rightarrow \Omega_{obj} = A_{obj}$<br>- If $A_{obj} \geq 1$ arcsec$^2 \Rightarrow \Omega_{obj} = 1\ arcsec^2$<br>Sky emission: $\Omega_{obj,sky} = 1$ arcsec$^2$ | SNR per arcsec$^2$, in selected spectral aperture | | SNR per arcsec per Å | $N_{pix}$ in 1 y-projected arcsec$^2$:<br>$n_{pix,y} =$<br>FLOOR$[1arcsec^2/A_{fiber}] \times [2 \times R_{eff,fiber}/PS]$ | |
| | | 1 x-pixel:<br>$\Delta\lambda = D$ | | | | |

| | | | | |
|---|---|---|---|---|
| | | $n_{pix,x} = 1$ | | |
| | Source emission in 1 y-pixel of a projected fiber(***):<br>- *If FWHM* $< 2R_{fiber} \Rightarrow \Omega_{obj}=A_{seeing}$<br>- *If FWHM* $\geq 2R_{fiber} \Rightarrow$ S*(in 1 y-pixel) = S(in 1 spaxel /[no. Pixels in one voxel] if uniform distribution.*<br>*If not, 32.82% in the fibers of 100 micron divided into the number of pixels of the FWHM in the spectral direction.*<br>Sky emission: $S_{sky}$*(in 1 y-pixel)* = $S_{sky}$ *(in 1 spaxel)/[16* pix/spx*]* | SNR in 1 detector pixel | 1 y-pixel: $n_{pix,y} = 1$ | |

Notes:

(*) The projected area of the extended source is assumed to be circular.

(**) The area of all the required fibers to ensure a complete coverage of the source will be noted $A(N_{fibers})$ hereafter. In this case, this area is: $A(N_{fibers})=A_{fiber}\, N_{fibers}$, where $N_{fibers}$ computes the integer number of fibers required to cover the source. We will note as "FLOOR" to the function that returns the nearest and highest integer of a given decimal value, then: $N_{fibers}$ = FLOOR$(A_{obj}/A_{fiber})$.

(***) In this case, the total integer number of fibers required to cover a seeing disk is also assumed: $A(N'_{fibers})=A_{fiber}\, N'_{fibers}$, where now $N'_{fibers}$=FLOOR$(A_{seeing}/A_{fiber})$.

# 8. MEGARA EXPECTED PERFORMANCE

## 8.1. Limiting magnitudes and fluxes

In *Table 10* we show the limiting magnitudes and fluxes to get SNR=10 in one MEGARA voxel, considering 1 hour of exposure time, obtained with the MEGARA ETC v.0.4.0 in all the proposed VPHs. The input spectrum is assumed to be flat.

| | Continuum limiting V-band magnitudes(*) to get SNR=10 in one voxel for $t_{exp}$=3600 s | | Line limiting fluxes(*),(***) to get SNR=10 in one voxel for $t_{exp}$=3600 s | |
|---|---|---|---|---|
| VPH in LCB or MOS mode | Point source (mag) | Extended source(**) (mag/arcsec$^2$) | Point source (erg/s/cm$^2$/Å) | Extended source(**) (erg/s/cm$^2$/Å/arcsec$^2$) |
| HR-R | 22.7 | 21.2 | 1.2e-18 | 4.4e-18 |
| HR-I | 22.0 | 20.5 | 1.1e-18 | 4.4e-18 |
| MR-U | 21.7 | 20.2 | 3.5e-18 | 1.4e-17 |
| MR-UB | 22.2 | 20.7 | 2.6e-18 | 1.0e-17 |
| MR-B | 22.5 | 21.0 | 2.1e-18 | 8.2e-18 |
| MR-G | 22.7 | 21.2 | 1.8e-18 | 7.1e-18 |
| MR-V | 22.9 | 21.4 | 1.5e-18 | 6.0e-18 |
| MR-VR | 23.0 | 21.6 | 1.4e-18 | 5.4e-18 |
| MR-R | 23.1 | 21.6 | 1.3e-18 | 5.0e-18 |
| MR-RI | 22.1 | 20.7 | 1.2e-18 | 4.8e-18 |
| MR-I | 22.2 | 20.7 | 1.1e-18 | 4.5e-18 |
| MR-Z | 22.2 | 20.7 | 1.3e-18 | 5.3e-18 |
| LR-U | 22.5 | 21.0 | 3.2e-18 | 1.3e-17 |
| LR-B | 23.2 | 21.7 | 1.7e-18 | 6.7e-18 |
| LR-V | 23.5 | 22.0 | 1.3e-18 | 5.0e-18 |
| LR-R | 23.7 | 22.2 | 1.1e-18 | 4.2e-18 |
| LR-I | 22.7 | 21.2 | 9.5e-19 | 3.8e-18 |
| LR-Z | 22.6 | 21.1 | 1.2e-18 | 4.6e-18 |

Notes:
(*) Assuming dark night with seeing of *FWHM(X=1) = 0.5"* at zenith and *X=1*.
Total coverage in one pointing (overheads are not being considered). Number of sky fibers set to default in each mode.
(**) Assuming target size = 1arcsec$^2$.
(***) Assuming non-resolved lines (i.e., FWHM set by the VPH), and a line wavelength placed at the center of the VPH wavelength range. Negligible continuum assumed: V(continuum)=30 mag.

***Table 10:** MEGARA expected performance in LCB/MOS mode.*

MEGARA is expected to detect point sources with SNR=10 in one voxel with a continuum magnitude[(14)] V=22.7, 23.1, and 23.7 mag in high-, medium-, and low-resolution respectively, in one hour in the wavelength range covered by the *R*-band. Similar performances are expected in the *V* band, and ~0.7 mag brighter in the *B* range. The performance in both extremes of the total wavelength range covered by MEGARA is a bit lower (see *Figure 3*), due to the lower total efficiency expected in them (this affects to the *U* and *I*-band ranges, consult *Table 10*). For extended sources, MEGARA is expected to reach SNR=10 in one voxel for sources as faint as V=21.2, 21.6, and 22.2 mag/arcsec$^2$ in 1h-long exposures.

MEGARA is expected to detect line fluxes of point sources with SNR=10 in one voxel as faint as *f*=4.4e-18, 5.0e-18, and 4.2e-18 c.g.s. in high-, medium-, and low-resolution respectively, for an exposure of 1h, at the central wavelength of the VPHs HR-R, MR-R, and LR-R respectively. For extended sources, the limiting fluxes for SNR=10 rise by a factor of ×4 approximately.

## 8.2. Comparison with other existing facilities

GTC+MEGARA shall fill a gap currently existing of a IFS facility providing high spectral resolution, wide FoV, and high sensitivity at the same time (see the “MEGARA Detailed Design: Instrument Overview” document). This makes difficult to compare the expected performance of MEGARA with other facilities, as no instrument with capabilities similar to those of MEGARA exists or is under design. Therefore, we give a comparison below of the improved performance expected for the MEGARA LCB, as compared to the configurations of some instruments providing similar spectral resolutions (Gemini/GMOS, CAHA/PPAK, VLT/FLAMES, and VLT/XSHOOTER). Analogous spatial and spectral resolution elements have been assumed in both focal planes.

GMOS are two twin spectrographs at both 8.1m Gemini telescopes, which offer long-slit, multi-object and fiber-fed IFS capabilities[15]. With a FoV smaller than MEGARA LCB by a factor of 4 and a similar wavelength range, each GMOS spectrograph provides better spatial resolution (down to 0.08"/pixel), but lower maximum spectral resolution than MEGARA (see *Table 11*). GMOS spectrographs offer a configuration with a dispersion and wavelength coverage similar to that of the LR-V VPH of MEGARA (~0.26 Å/pixel): the grating B1200 combined with the OG515 filter. We have used the GMOS ETC[16] in order to compare the output SNRs obtained with this configuration with that obtained with MEGARA LCB using the LR-V VPH in equivalent physical elements onto the detectors of both instruments. Accounting for the similar transmissions of both instruments and their different plate scales (which imply that the SNR obtained with MEGARA at each detector pixel is a factor of ~8.5 higher than that of GMOS just because of the ratio between their sky-projected fiber diameters), we have found that the obtained SNRs are compatible with a better performance by MEGARA by ~25-30% in SNR,

[14] All magnitudes in the MEGARA ETC and in this user guide are in the Vega system.

[15] GMOS Integral Field Spectroscopy, Gemini Observatory web pages:
http://www.gemini.edu/node/10625?q=node/10372

[16] GMOS integration time calculator. M. Dillman, 2009:
http://sciopsedit.gemini.edu/sciops/instruments/integration-time-calculators/gmosn-itc

for point and extended sources, as well as for continuum and line cases. This improvement is basically due to the higher collecting area of GTC compared to that of the Gemini telescope. However, note that both instruments offer different capabilities: while GMOS provides high spatial resolution, low spectral resolution, and a small FoV, MEGARA will provide intermediate spatial resolution, low-to-high spectral resolution, and a wider FoV. Hence, although each instrument is optimized for different scientific purposes, GTC+MEGARA will be slightly more efficient than GMOS.

PPAK is a fiber-IFU mounted at the 3.5m telescope of Calar Alto Observatory (CAHA). With a FoV wider than the one of the MEGARA LCB by a factor of ~25 and covering the same wavelength range, their fibers are wider by more than a factor of ×4 than those of the LCB[17] (see *Table 11*). Comparing the output SNRs in equivalent cases for both instruments for a point source[18] and considering that the SNR at each detector pixel of PPAK is a factor of ×4 higher than in one projected pixel of the MEGARA LCB (because of the bigger projected section of a PPAK fiber), we have checked that MEGARA will improve the SNR obtained with PPAK by a factor of ~3.5, considering analogous spatial and spectral elements in both instruments. The different collecting areas of GTC and CAHA 3.5m telescopes are responsible of a factor of ×2.9, while the better transmission expected for MEGARA (nearly twice that of PPAK in the whole wavelength range) explains the rest of SNR enhancement. Therefore, MEGARA will achieve a given SNR per arcsec and per Å in a given source using 8 times less exposure time than PPAK, providing better spatial and spectral resolutions at the same time (here we do not account for the 3-pointings dithering required by PPAK to fill the gaps between fibers, which would rise this factor even further).

| | GTC/ MEGARA LCB | Gemini-N/ GMOS IFU | CAHA3.5m/ PPAK | VLT/ FLAMES (GIRAFFE +ARGUS IFU) | VLT/ XSHOOTER |
|---|---|---|---|---|---|
| Telescope Ø (m) | 10.4 | 8.1 | 3.5 | 8.2 | 8.2 |
| FoV | 12.5"x11.3" | 5"×7" | 1.2'×1' | 11.5"×7.3" | 4"×1.8" |
| Spatial Resolution | 0.62"/fibre | 0.31"/fibre | 2.7"/fibre | 0.52"/fibre | 0.16"/pixel |
| Spectral resolution | 5500 - 17,000 | 6000 | 3000 - 14,000 | 11,000 -35,000 | 3000 - 18,000 |
| Wavelength range (Å) | 3700 - 9700 | 4000 - 11,000 | 2500 - 10,000 | 3700 - 9500 | 3000 - 25,000 |

***Table 11:*** *Comparison of the main characteristics of GTC+MEGARA with those offered by other existing facilities.*

[17] PMAS Technical Overview, CAHA web pages:
http://www.caha.es/pmas/PMAS_OVERVIEW/pmas_overview.html#IFU

[18] CAHA/PMAS exposure time calculator. S. Sánchez, 2006:
http://www.caha.es/sanchez/pmas/calculator/pmas_etc.php

FLAMES/GIRAFFE is a spectrograph located at one of the 8.2m telescopes of VLT (the UT2), that allows an IFU configuration through ARGUS, an array of micro-lenses feeding a bundle of fibers. FLAMES can do medium- and high-resolution spectroscopy (up to R=46,000) in small FoV at optical wavelengths, so it is not directly comparable to MEGARA either[19]. The spatial resolution is slightly better than that of MEGARA LCB (see *Table 11*) and the transmission is worse by a factor of ×2, depending on the wavelength. FLAMES/GIRAFFE+ARGUS offers two FoVs, the widest being smaller than the MEGARA LCB. One of its configurations (LR5) provides a similar dispersion and wavelength coverage as MEGARA LCB with the MR-V VPH. Comparing the output SNRs obtained with both instruments in a point source and accounting for the different projected fiber sizes[20], we have found that the MEGARA would provide an enhancement by a factor of ~1.6 in the SNR of equal resolution elements. This improvement is due to the difference of telescope collecting areas and to the higher transmission expected for MEGARA, basically. Therefore, even being facilities providing different and complementary capabilities, GTC+MEGARA is slightly more efficient than the VLT instrument GIRAFFE+ARGUS in analogous cases.

XSHOOTER is a multi-wavelength medium resolution spectrograph mounted at the VLT UT2 Cassegrain focus[21]. It consists of 3 arms, each one being an independent cross dispersed echelle spectrograph with optimized optics, dispersive elements, and detectors for different wavelength ranges. The incoming light is split into the three different spectrographs/arms through 2 dichroics. The two arms that overlap in spectral range with that of MEGARA are the UVB (300-559.5 nm) and the VIS (559.5-1024 nm) arms. XSHOOTER covers ~20 times less area in one pointing than the MEGARA LCB, but has better spatial resolution (see *Table 11*). It offers spectral resolutions very similar to those offered by MEGARA for wavelengths longer than 5600 Å (R~5400-18,200 in VIS), but not as high in the blue range (R~3300-9900 in UVB). We have compared the total SNRs in a spectral resolution element expected for an A0V star with V=20 mag obtained with both instruments for 1 hour of exposure time, using configurations that provide equivalent spectral resolutions at similar wavelengths[22]. We have assumed that the observations have been taken during a dark night with a seeing FWHM=1.0” at airmass X=1. The results in *Table 12* show that GTC+MEGARA shall provide SNRs per Å and arcsec in a given source a factor of ~2-3 higher than XSHOOTER for analogous cases, which is a reasonable result accounting for the difference in telescope collecting areas and in total efficiency (higher in MEGARA by a factor of ~2-5 typically). Therefore, GTC+MEGARA shall

---

[19] FLAMES/GIRAFFE Spectrograph description, VLT web pages:
http://www.eso.org/sci/facilities/paranal/instruments/flames/inst/Giraffe.html

[20] FLAMES/GIRAFFE Exposure Time Calculator, version 3.2.7 (March 4, 2009):
http://www.eso.org/observing/etc/bin/gen/forms?INS.NAME=GIRAFFE++INS.MODE=spectro

[21] VLT/XSHOOTER ESO webpage:
http://www.eso.org/sci/facilities/paranal/instruments/xshooter/index.html

[22] VLT/XSHOOTER Echelle Spectroscopy Mode, version 3.2.1**3** Exposure Time Calculator:
http://www.eso.org/observing/etc/bin/gen/form?INS.NAME=X-SHOOTER+INS.MODE=spectro

cover much wider area than XSHOOTER, providing higher spectral resolution and higher expected performance, although the later one offers a factor of ~3-4 better spatial resolution than the former one.

In conclusion, the expected performance of GTC/MEGARA as simulated by the MEGARA ETC demonstrates that it shall provide with unique spectroscopic capabilities to GTC in the whole optical range, not covered by any other existing facility at the present, that will allow the scientific community to carry out high-quality observations for high-impact scientific projects.

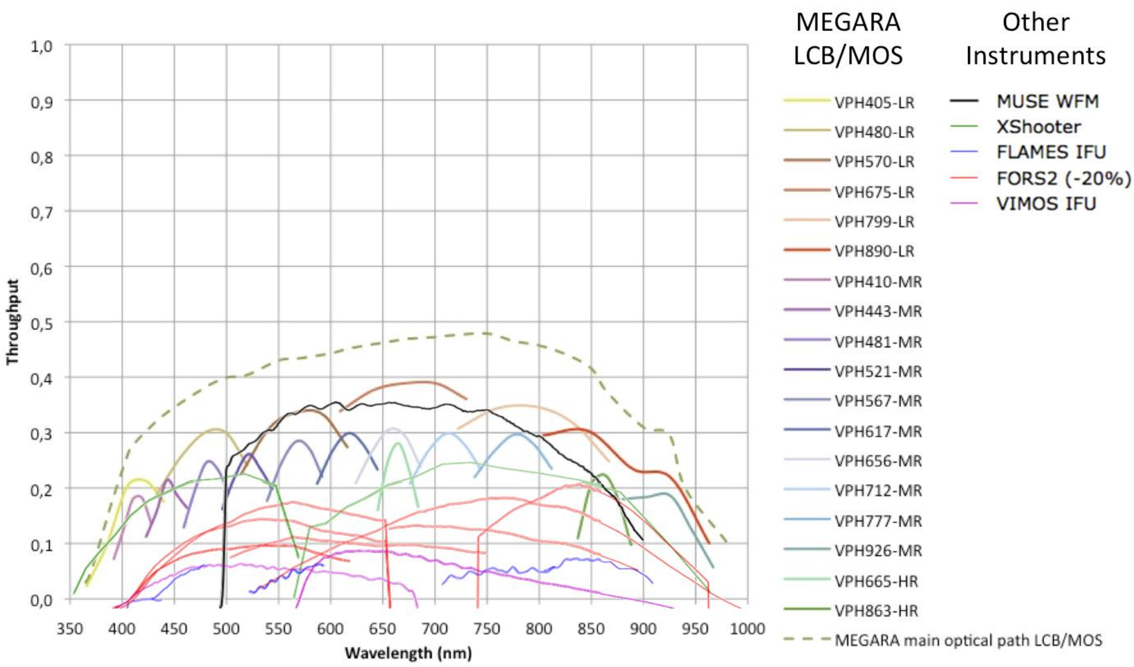


***Figure 14:*** *Comparison of GTC/MEGARA throughput at different wavelengths with other existing facilities.*

| **VLT+XSHOOTER configuration** | | | | **GTC+MEGARA LCB equivalent configuration** | | | | **MEGARA-to-XSHOOTER improvement factor of the SNR in 1 spectral FWHM** | |
|---|---|---|---|---|---|---|---|---|---|
| VIS arm R = 6700 @ 5595 – 10,240 Å slit =1.2" - FWHM=7.9 pix - 1×1binning | | | | VPHs R=6250 @ 5595 – 10,240 Å Spectral FWHM = 3.5 pix | | | | | |
| $\lambda_{Blaze}$ (Å) | SNR in 1 spectral pixel | SNR in 1 spectral FWHM | Eff (%) | VPHs | $\lambda_{central}$ (Å) | SNR in 1 spectral FWHM | Eff (%) | Expected from differences in telescope diameter and efficiency | Obtained from the estimates of ETCs |
| 6821 | 11 | 31 | 11 | LR-R | 6749 | 97 | 35 | ×2.2 | ×3.1 |
| 8602 | 8 | 21 | 11 | LR-I | 8650 | 55 | 15 | ×1.4 | ×2.6 |
| | | | | | | | | | |
| VIS arm R = 10,600 @ 5595 – 10,240 Å slit =0.7" - FWHM=4.9 pix - 1×1binning | | | | VPHs R=11,000 @ 5595 – 10,240 Å range Spectral FWHM = 3.5 pix | | | | | |
| $\lambda_{Blaze}$ (Å) | SNR in 1 spectral pixel | SNR in 1 spectral FWHM | Eff (%) | VPHs | $\lambda_{central}$ (Å) | SNR in 1 spectral FWHM | Eff (%) | Expected from differences in telescope diameter and efficiency | Obtained from the estimates of ETCs |
| 5680 | 9 | 20 | 5.7 | MR-V | 5667 | 63 | 35 | ×2.8 | ×3.2 |
| 6295 | 9 | 20 | 6.8 | MR-VR | 6170 | 63 | 35 | ×2.5 | ×3.2 |
| | | | | | | | | | |
| UVB arm R = 6200 @ 3000 – 5595 Å slit=0.8" - FWHM=5.2 pix - 1×1 binning | | | | VPHs R=6250 @ 3000 – 5595 Å Spectral FWHM = 3.5 pix | | | | | |
| $\lambda_{Blaze}$ (Å) | SNR in 1 spectral pixel | SNR in 1 spectral FWHM | Eff (%) | VPHs | $\lambda_{central}$ (Å) | SNR in 1 spectral FWHM | Eff (%) | Expected from differences in telescope diameter and efficiency | Obtained from the estimates of ETCs |
| 4145 | 20 | 45 | 8.1 | LR-U | 4051 | 36 | 6 | ×1.0 | ×0.8 |
| 4660 | 20 | 45 | 8.5 | LR-B | 4800 | 70 | 10 | ×1.4 | ×1.5 |
| 5560 | 11 | 25 | 3 | LR-V | 5700 | 92 | 35 | ×4.0 | ×4.0 |
| | | | | | | | | | |

**Comments to Table:**

1. The SNRs are computed integrating spatially for the whole source.
2. The MEGARA spectral resolutions are computed using the spectral FWHM of the MEGARA LCB as δλ.
3. The efficiencies (Eff) of XSHOOTER refer to the total efficiency, including the slit loss and atmospheric extinction. The efficiencies of MEGARA include telescope+instrument flux losses and atmospheric transmission at La Palma observatory.
4. A dark night with a seeing FWHM=1.0" and airmass X=1 have been assumed in both cases.
5. The improvement factors of the SNR obtained with MEGARA compared to XSHOOTER have been estimated in two ways: accounting for the efficiency and telescope diameter differences, and considering the estimates obtained with the ETCs of both instruments (compare the two last columns of the Table). The agreement between both estimates is worse at redder wavelengths. This is due to the existence of noticeable atmospheric absorption lines at longer wavelengths, considered differently in each ETC.

***Table 12:*** *Comparison of the continuum SNR expected for a point source with V=20 mag, for 1 hour of integration time in VLT+XSHOOTER and GTC+MEGARA, using configurations with similar spectral resolutions at similar characteristic wavelengths.*

# 9. INDEX OF FIGURES

# 10. INDEX OF TABLES